Precambrian Research 319 (2018) 79–95

Contents lists available at ScienceDirect

Precambrian Research

journal homepage: www.elsevier.com/locate/precamres

The Tonian-Cryogenian transition in Northeastern Svalbard

Galen P. Halverson[a], Marcus Kunzmann[b,c], Justin V. Strauss[d], Adam C. Maloof[e]

[a] Dept. of Earth and Planetary Sciences/Geotop, McGill University, 3450 University Street, Montréal, QC H3A 0E8, Canada
[b] CSIRO Mineral Resources, Australian Resources Research Centre, Kensington, WA 6151, Australia
[c] Northern Territory Geological Survey, Darwin, NT 0800, Australia
[d] Dept. of Earth Sciences, Dartmouth College, HB6105 Fairchild Hall, Hanover, NH 03755, USA
[e] Department of Geosciences, Princeton University, Guyot Hall, Washington Road, Princeton, NJ 08544, USA

ARTICLE INFO

Keywords:
Neoproterozoic
Stratigraphy
Carbonates
Carbon isotopes
Strontium isotopes
Redox proxies
Laurentia

ABSTRACT

The Neoproterozoic stratigraphic succession in northeastern Svalbard is uniquely important in documenting the evolution of Neoproterozoic life, seawater chemistry, and paleoenvironments. This contribution focuses on the stratigraphic and geochemical records spanning from the late Tonian to the onset of Cryogenian glaciation in the Hecla Hoek Series, with the purpose of informing debates on the subdivision of the Neoproterozoic time scale, the cause of the descent into the first snowball ice age, and the tempo of Neoproterozoic oxygenation. This interval is represented by the Kinnvika Member of the uppermost Akademikerbreen Group and the Russøya Member of the Elbobreen Formation, lowermost Polarisbreen Group. These units record the demise of the long-lived, stable Akademikerbreen carbonate platform in the East Svalbard basin. The upper Russøya Member preserves a deep negative carbon isotope anomaly that has been linked mechanistically to the onset of Cryogenian cooling. This anomaly was previously correlated with the so-called Islay negative carbon isotope anomaly in Scotland. Here we propose a revised correlation of the latest Tonian section in Svalbard with equivalent-aged but better dated successions in northern Laurentia using sequence stratigraphy and carbon and strontium isotope chemostratigraphy. These correlations provide a means for calibrating the Tonian-Cryogenian transition interval in Svalbard and suggest that the upper Russøya negative carbon isotope anomaly significantly predates the onset of Cryogenian glaciation, with ca. 20 million years of missing record beneath the disconformity at the base of the overlying glaciogenic Petrovbreen Member. This anomaly may be the older of two late Tonian negative carbon isotope anomalies of similar magnitude.

1. Introduction

The Svalbard archipelago is located on the northwestern corner of the Barents Shelf, north of mainland Norway. The islands collectively comprise three pre-Devonian provinces with distinct geological histories that assembled north of Greenland late in the Caledonian orogeny. These provinces (Fig. 1) were subsequently displaced to the east (relative to Greenland) along with the remainder of Svalbard during Cenozoic opening of the North Atlantic Ocean (Harland et al., 1992; Gee and Page, 1994). Neoproterozoic strata are well known in both in the Southwestern and Eastern provinces (Harland et al., 1993) and may occur in the intervening Northwestern Province as well (Pettersson et al., 2009). The Neoproterozoic rocks in the Southwestern Province are heavily deformed, but glacial deposits are clearly identified there (Harland et al., 1992; Bjørnerud, 2010). The Neoproterozoic strata in the Eastern Province, in contrast, are exceptionally well preserved by Proterozoic standards and have been the subject of many studies that have been central in elucidating Neoproterozoic Earth history (e.g. Harland, 1964; Fairchild and Hambrey, 1984; Knoll et al., 1986; Kaufman et al., 1997; Bao et al., 2009; Benn et al., 2015).

The Neoproterozoic succession in the Eastern Province is part of the upper Hecla Hoek Series (Harland and Wilson, 1956), which outcrops in nunataks and coastal sections in northeastern Spitsbergen and northwestern Nordaustlandet (Fig. 1). These strata are subdivided into the Veteranen, Akademikerbreen, and Polarisbreen groups (Fig. 2). Collectively, these rocks provide an unusually complete sedimentary record spanning ca. 850 to 600 Ma (Halverson et al., 2005), with the only significant disconformities corresponding to the two Cryogenian glaciations within the middle Polarisbreen Group.

The lower to middle Tonian-aged Veteranen Group comprises dominantly siliciclastic rocks, with minor shallow-water carbonates. The ~2 km-thick, middle–upper Tonian Akademikerbreen Group is almost exclusively carbonate and records the entirety of the ca. 810–800 Ma Bitter Springs carbon isotope anomaly (BSA; Halverson et al., 2007b; Macdonald et al., 2010; Swanson-Hysell et al., 2012; Swanson-Hysell et al., 2015). The conformably overlying Polarisbreen

E-mail address: galen.halverson@mcgill.ca (G.P. Halverson).

https://doi.org/10.1016/j.precamres.2017.12.010
Received 6 July 2017; Received in revised form 30 October 2017; Accepted 3 December 2017
Available online 09 December 2017
0301-9268/

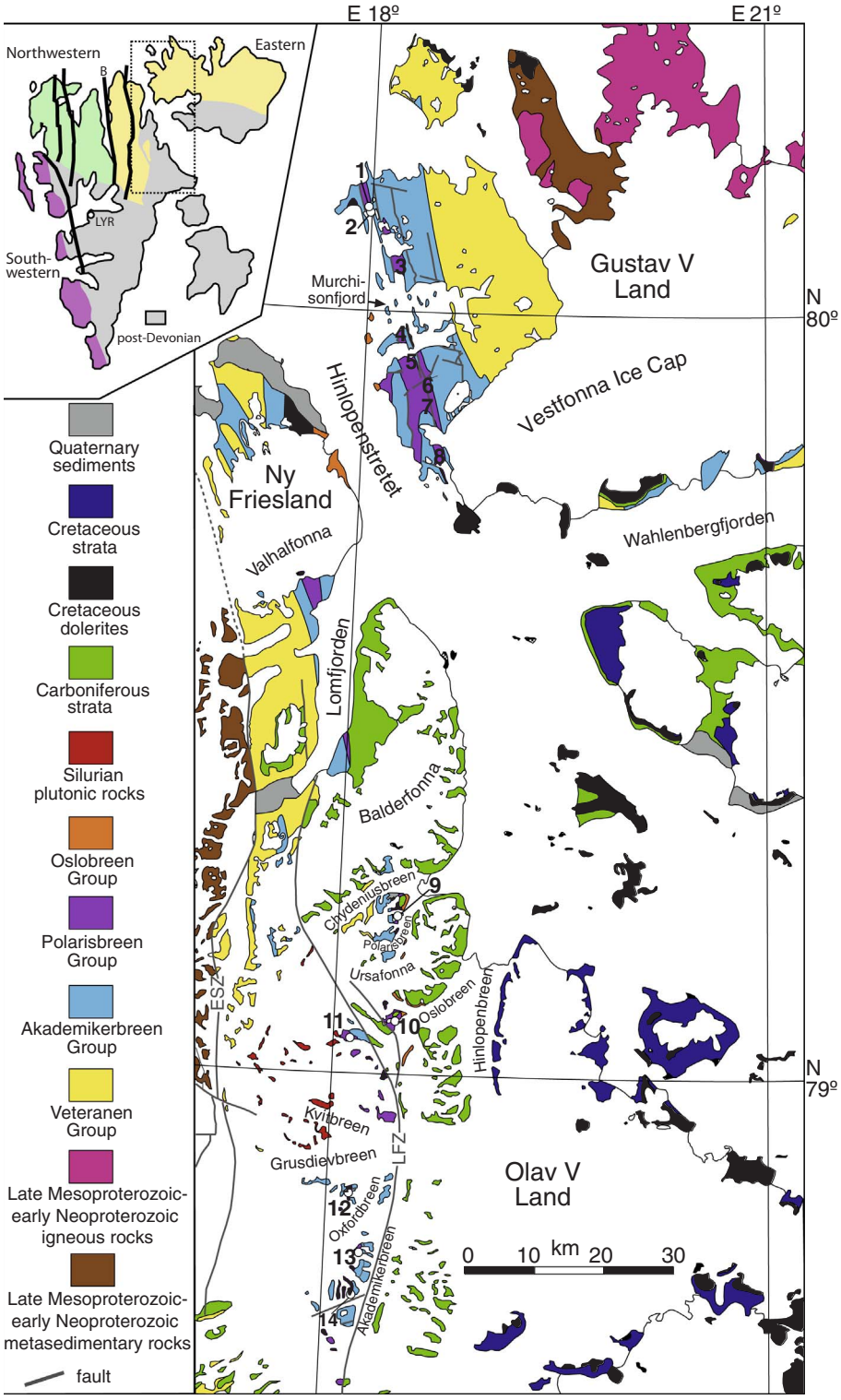

Fig. 1. Geological map of northeastern Spitsbergen and northwestern Nordaustlandet (modified from Halverson, 2011) showing the distribution of the Hecla Hoek Series (Veterane through Oslobreen groups) in the Eastern Province of Svalbard. Location numbers on map are keyed to stratigraphic logs in subsequent figures: (1) Langruneset, (2) Bråvika, (3) Kinnvika, (4) Søre Russøya, (5) Sveanor, (6) Liljequistøgta, (7) Kalkberget, (8) Gimleodden, (9) Dracoisen, (10) Ditlovtoppen, (11) Doleritfjellet, (12) Klofjellet, (13) Macdonaldryggen (from Harland et al., 1993), (14) Backlundtoppen. Inset map (modified from Mazur et al., 2009) shows the three provinces comprising pre-Devonian Svalbard. The Eastern Province is juxtaposed with the Northwestern Province along the strike-slip Billefjorden Fault Zone (B). LYR = Longyearbyen.

Group comprises mixed siliciclastics and carbonates, but locally, the pre-Cryogenian interval of the Polarisbreen Group (Russøya Member) is dominantly composed of carbonates and preserves a deep negative $\delta^{13}C$ anomaly that was previously correlated with the so-called Islay anomaly of Scotland (Hoffman et al., 2012). The basal Ediacaran Dracoisen cap dolostone occurs across the outcrop belt and serves as a useful chronostratigraphic marker (Harland et al., 1993; Halverson et al., 2004) that can be confidently assigned an age of ca. 635 Ma (Hoffmann et al., 2004; Condon et al., 2005; Calver et al., 2013).

The purpose of this contribution is to provide an overview of the latest Tonian stratigraphy in northeastern Svalbard in the context of the current debates over the trigger mechanism for the onset of the first Cryogenian glaciation (e.g., Cox et al., 2016; Macdonald and Wordsworth, 2017) and the link between Neoproterozoic oxygenation and biospheric evolution, as well as to inform the deliberations over definition of the basal Cryogenian boundary (i.e., Global Stratotype Section and Point—GSSP; Shields-Zhou et al., 2016). Specifically, we synthesize previously published and new stratigraphic, sedimentological, chemostratigraphic, redox and limited paleontological data and observations spanning the Akademikerbreen-Polarisbreen transition in

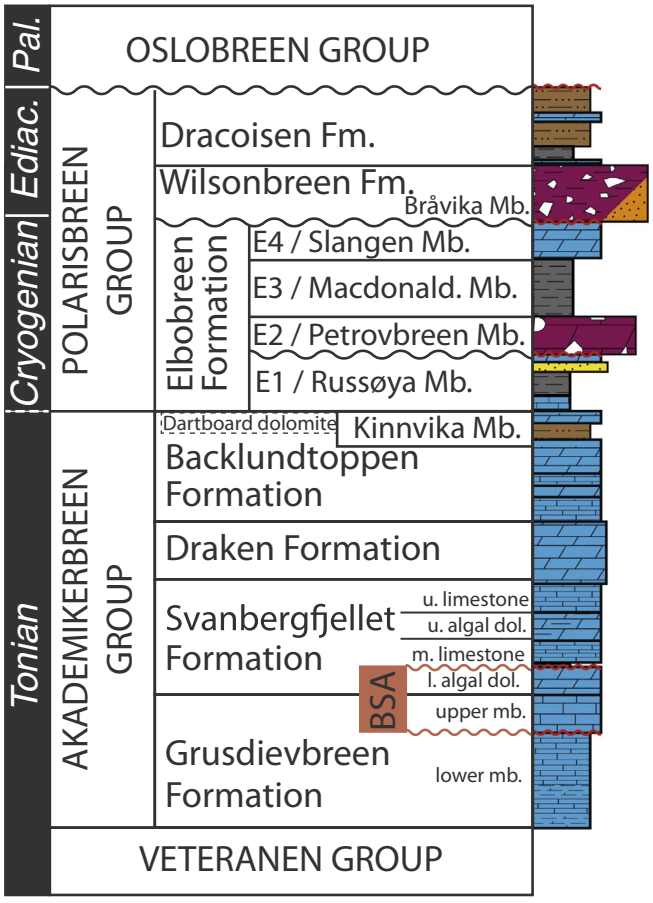

Fig. 2. Stratigraphic nomenclature for the Tonian Akademikerbreen Group and Tonian–Ediacaran Polarisbreen Group used in this paper. Note that the "Kinnvika Member," introduced by Halverson et al. (2004), is spelled differently here to conform to more recent spelling of the eponymous station in the Murchisonfjord region of Nordaustlandet. BSA = Bitter Springs Anomaly. Informal members of the Svanbergfjellet are as described in text and introduced by Knoll and Swett (1990). Ediac. = Ediacaran. Pal. = Paleozoic.

Svalbard, with an emphasis on establishing the stratigraphic and temporal context of the Russøya negative carbon isotope anomaly. No direct ages have been obtained on the Neoproterozoic strata or their equivalents in East Greenland, but correlation of the Akademikerbreen-Polarisbreen transition strata with analogous sequences in northern Canada provides useful age constraints that can be used to calibrate the late Tonian record in Svalbard and assess its level of completeness leading into to the Cryogenian period.

2. Paleogeographic context

The similarity between the Neoproterozoic stratigraphic successions of the Eastern Terrane of Svalbard and East Greenland Caledonides (i.e., the Eleonore Bay Supergroup and Tillite Group) is cited as evidence that these two regions were contiguous parts of eastern Laurentia in the Neoproterozoic (Harland and Gayer, 1972; Fairchild and Hambrey, 1995; Hoffman et al., 2012) (Fig. 3). Both regions were deformed and locally intruded by felsic igneous rocks during the Scandian phase of the Caledonian orogeny (ca. 440–410 Ma). Hence, most paleogeographic reconstructions directly juxtapose the Eastern Province and the East Greenland Caledonides along the eastern margin of Laurentia during the Neoproterozoic (e.g., Harland and Gayer, 1972; Maloof et al., 2006). The Southwestern Province, in contrast, shows affinities with northern Greenland (Harland and Wright, 1979; Ohta et al., 1989; Gee et al., 2004) and/or Baltica (Gasser and Andresen, 2013; Majka et al., 2014). The basement to the Old Red Sandstone in the Northwestern Province is less well understood, but latest Mesoproterozoic to earliest Neoproterozoic metasediments in the province (Pettersson et al., 2009) indicate an affinity with the Grenville or Valhalla orogens (cf. Cawood et al., 2010).

It follows from the assumed conjugate relationship between the Eastern Province (hereafter referred to as East Svalbard) and East Greenland that the former traveled northward via sinistral strike-slip displacement to its pre-Cenozoic position north of Greenland during the Silurian-Devonian (Harland and Wright, 1979; Gasser and Andresen, 2013), perhaps as a consequence of escape tectonics (Ohta et al., 1994). However, the affinity and paleogeography of East Svalbard (Fig. 3) remains controversial (Johansson et al., 2005), and it could have been located anywhere along the eastern margin of Greenland. Although the Neoproterozoic stratigraphic succession in East Svalbard is unequivocally similar to the succession in East Greenland, the two regions may have lay along depositional strike (i.e., on the same margin) rather than having been on opposing sides of a rift (cf. Harland and Gayer, 1972). This possibility allows that East Svalbard may have been located much further north than the East Greenland Caledonides (in present coordinates). In either case, the stratigraphic successions and geometries in both basins appear to be consistent with a non-magmatic rifting phase (i.e., Veteranen Group in East Svalbard), followed by a thermal subsidence phase (Akademikerbreen Group) of the basin, with deposition occurring in tropical latitudes (Maloof et al., 2006). In the recent model that places East Svalbard in the foreland to the Valhalla accretionary origin on the margin of Rodinia (Cawood et al., 2010; Cawood et al., 2016), the basin represents a post-orogenic rift. However, given that the onset of Veteranen Group deposition must significantly predate ca. 810 Ma (the onset of the Bitter Springs anomaly), it is unlikely that the origin of the East Svalbard-East Greenland basin was directly related to latest Neoproterozoic opening of the Iapetus Ocean.

3. Neoproterozoic stratigraphy of NE Svalbard

The Neoproterozoic stratigraphic succession in northeastern Spitsbergen is subdivided into the Veteranen, Akademikerbreen, and Polarisbreen groups (Fig. 2). Whereas a different nomenclature has historically been used for the equivalent strata in Nordaustlandet (e.g,Flood et al., 1969), correlation of the Akademikerbreen–Polarisbreen strata across Hinlopenstretet (Fig. 1) is unambiguous, and it has become the convention to use the better known stratigraphic nomenclature from Spitsbergen (Fairchild and Hambrey, 1995; Halverson et al., 2005). This convention is followed in this manuscript.

3.1. Veteranen Group

The Veteranen Group consists of a thick package of mixed sandstone, siltstone, shale and carbonate deposited predominantly or perhaps entirely within a marginal marine environment (Wilson, 1958). The Veteranen Group has not been studied in detail and its base is typically either unexposed or a tectonic contact. The most complete section of the Veteranen Group is found on the south side of Faksevågen in northwestern Lomfjorden (Fig. 1). Here, the Veteranen Group is approximately 7.4 km thick, but it is base-truncated by a west-vergent Caledonian thrust (Dallmann et al., 2013). In Nordaustlandet, the equivalent of the basal Veteranen Group (variably the Meyerbukta Formation or Galtedalen Group; Sandelin et al., 2001) is thought to unconformably overly volcanigenic and metasedimentary strata (Gee and Tebenkov, 1996; Sandelin et al., 2001), which are intruded by subvolcanic granites and andesites. However, this contact is not well exposed (Sandelin et al., 2001). In situ U-Pb zircon ages on the volcanics and intrusives yield a range of ages of ca. 960–930 Ma (summarized in Johansson et al., 2005). Assuming that the contact between the Veteranen Group and the underlying basement is not tectonic here, these ages effectively provide the maximum age constraint on deposition of the Veteranen Group, and by extension, the origin of the

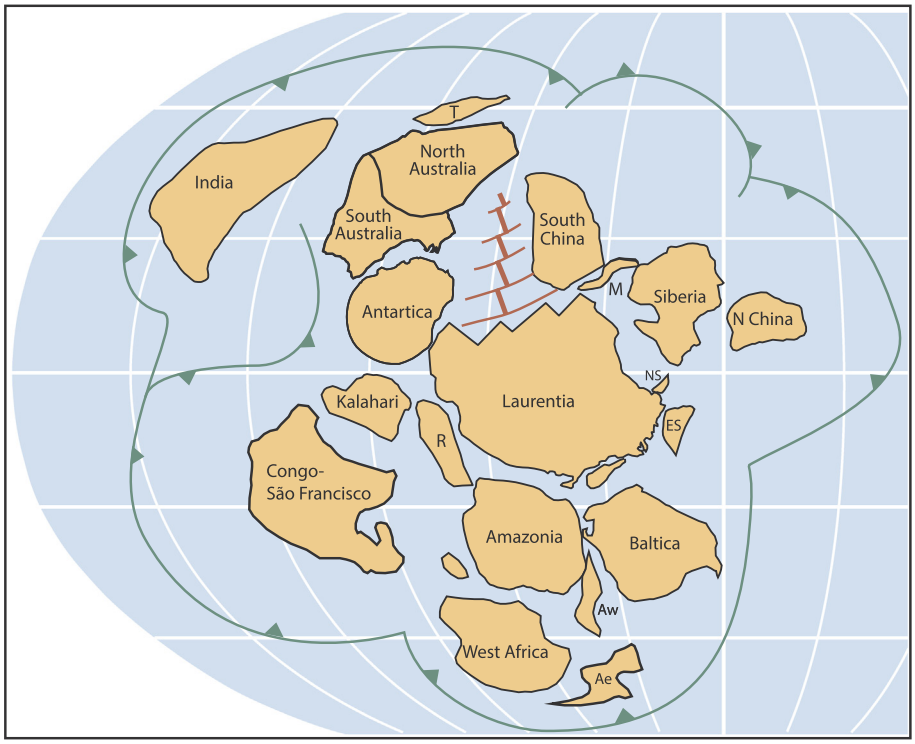

Fig. 3. 720 Ma paleogeographic reconstruction showing the location of the Eastern Svalbard Province (ES) placed alongside eastern Greenland in a hypothetical Rodinia configuration, modified from Cox et al. (2016) and Li et al. (2013). NS = North Slope subterrane; M = Mongolia; T = Tarim block; R = Rio Plata craton; Aw = western Avalon; Ae = eastern Avalon.

sedimentary basin filled by the Veteranen through Polarisbreen groups and their equivalents in East Greenland (coined the East Greenland-East Svalbard, or EGES basin by Hoffman et al., 2012).

3.2. Akademikerbreen Group

The Akademikerbreen Group (equivalent to the Hunnberg and Ryssø formations on Nordaustlandet) conformably overlies the Veteranen Group and is subdivided into (from base to top) the Grusdievbreen, Svanbergfjellet, Draken, and Backlundtoppen formations (Wilson, 1961; Knoll and Swett, 1990). Here we subdivide the units into six transgressive-regressive (T-R) sequences (T-R1 to T-R6) based on broad patterns of shoaling and deepening (Fig. 4). The sequence boundaries correspond to maximum regressive surfaces (MRS), such that the regressive systems tract (RST) is a composite of the highstand systems tract (HST), and where present, falling stage systems tract (FSST) and lowstand systems tract (LST).

The Akademikerbreen Group is up to 1900 m thick and is almost entirely composed of carbonates with only minor shale, siltstone, and sandstone. The Akademikerbreen Group is punctuated by only two subaerial unconformities, neither of which resulted in the development of significant erosional relief (Halverson et al., 2007b). As discussed in more detail below, the Akademikerbreen Group is thought to span from ca. 820–750 Ma. As such, it records a long-lived, stable carbonate platform.

The contact between the Veteranen Group and the overlying Akademi-kerbreen Group is transitional, manifested in a gradual increase in carbonate content in what is otherwise dominantly siltstone and shale of the upper Oxfordbreen Formation. In the Murchisonfjord region of Nordaustlandet, this transition coincides with a shoaling upwards sequence, represented by mud-cracked, finely laminated dolomitic siltstone and microbialaminite facies. The base of the Akademikerbreen Group records the beginning of the subsequent transgressive systems tract (TST) and the establishment of a storm-dominated carbonate ramp (Halverson et al., 2007b). This informally designated lower member of the Grusdievbreen Formation is ~450 m-thick and spans the first full T-R sequence (T-R1). The upper contact of this member is a subaerial disconformity (the G1 surface of Halverson et al. (2005)) that corresponds to the onset of the Bitter Springs Anomaly (BSA) (Fig. 4) in the Akademikerbreen Group. The ~250 m-thick upper Grusdievbreen Formation consists of red, white, and grey laminated to medium-bedded calcilutite to grainstone, with faint cross-bedding in places, minor microbial laminations, and rare authigenic talc (Halverson et al., 2007b; Tosca et al., 2011).

The contact with the overlying Svanbergfjellet Formation is poorly defined (Halverson et al., 2007b) but broadly corresponds to a shift from dominantly limestone to dominantly dolostone with more evident bedding and better preserved textures than the upper member of the Grusdievbreen Formation. These facies become increasingly organized into shallow water carbonate cycles up section. In the Murchisonfjord region of Nordaustlandet, these cycles are typically capped by stromatolites, which include the *Baicalia*, *Colonella*, and *Tungussia* form-genera (Knoll and Swett, 1990; Halverson et al., 2007b), which are variably associate with black talc. In Ny Friesland, these cycles include minor stromatolites but are dominantly made up of microbialaminite, grainstone, and rudstone facies inferred to have been deposited in a back-reef to supratidal setting. Collectively, this interval is informally referred to as the lower dolomite member (Knoll and Swett, 1990). The top of the member is a second subaerial unconformity (the S1 surface of Halverson et al., 2005), marked by brecciation, silicification and ferruginization (with the iron appearing to be derived from overlying shales). This surface corresponds to the end of the BSA and the top of T-R2.

The lower part of the overlying lower limestone member is marked by variegated red, green, grey, and black shales. The TST is thin to absent in this higher order sequence (T-R3a), and the regressive systems tract (RST) is capped by a distinctive *Minjaria-Conophyton* biostrome that occurs along the entire length of the outcrop belt in northeastern Svalbard (Knoll and Swett, 1990; Halverson et al., 2007a). The remainder of the member lies within T-R3b and consists of well bedded calcilutites and relatively organic-rich ribbon facies (i.e., irregular wavy laminated to thin-bedded lutite) limestones with abundant molar tooth structure and minor stromatolitic buildups. The overlying algal dolomite member comprises a series of shale to stromatolite cycles. The

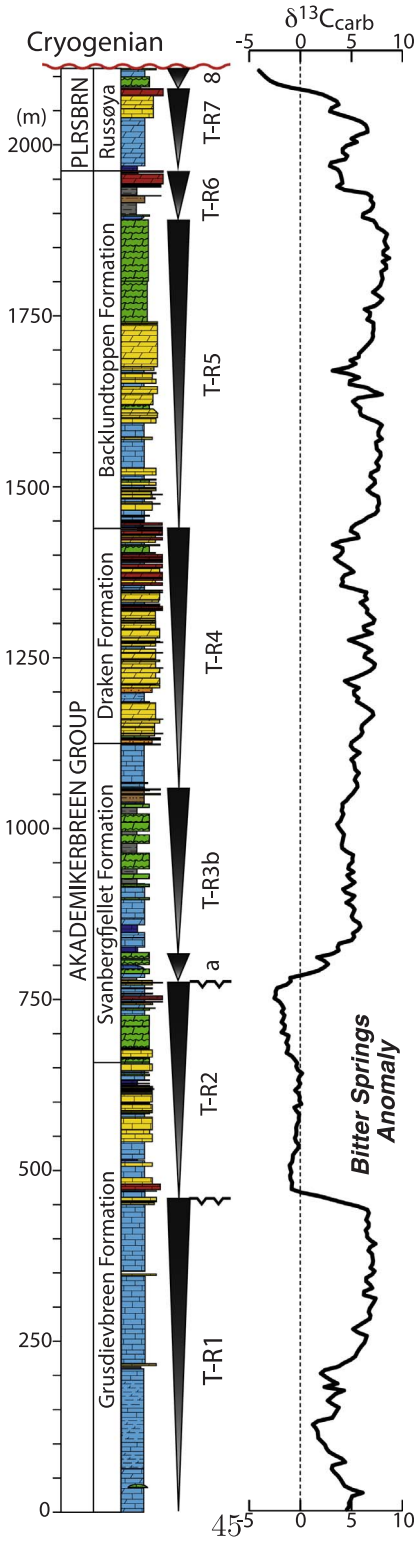

Fig. 4. Composite stratigraphic profile through the Akademikerbreen and lower Polarisbreen groups (i.e., the carbonate-dominated Tonian interval in northeastern Svalbard). Carbon isotope profile is a locally weighted regression (LOESS) fit of available carbon isotope data (from Halverson et al., 2005, 2007b; Cox et al., 2016). Shaded inverted triangles show the Transgressive-Regressive (T-R) sequences discussed in the text. See Fig. 5 for legend and supplementary information for data.

stromatolites are diverse, ranging from irregular, cabbage-shaped mounds (Knoll and Swett, 1990), to more coherent columnar and branching stromatolites forming biostromes that vary laterally in thickness. The intervening shales are commonly black and can be several meters thick, but the shales generally thin and are more commonly green and maroon in the southern part of the belt. The member forms the top of T-R3. Excellent examples of the compression macrofossils *Tawuia* and *Chuaria* occur in this unit (Butterfield et al., 1994).

The upper limestone member makes up the uppermost Svanbergfjellet Formation and consists of laminated to fine, parallel to wavy bedded, muddy calcimicrite to lutite, commonly of the ribbon facies (i.e., irregular to wavy bedded, thickly laminated to finely bedded carbonate), with interbedded wackestones, fine rudstones, and rare quartz arenite. This unit varies from > 100 m thick in southern exposures to absent or just a few meters thick in most Nordaustlandet sections. It defines the lower part of T-R4; the upper part of this sequence comprises the entire Draken Formation. The distinctively pale yellow to grey dolostone of the Draken Formation consists mainly of rudstone, grainstone (with common ooids), and microbialaminite, along with biohermal to biostromal stromatolites deposited in shallow subtidal to supratidal environments (Swett and Knoll, 1985; Fairchild et al., 1993). Beds of fine-grained quartiz arenite occur near the base of the Draken Formation in most sections.

The transitional contact between the Draken Formation and overlying Backlundtoppen Formation is the TST of T-R5. The lithofacies in this interval include interbedded yellow dolomitic grainstone and microbialaminite and black calcimicrite and lutite with lenses of ooids, commonly > 5 mm in diameter, and minor, irregular stromatolitic bioherms (Wilson, 1961; Swett and Knoll, 1989). In northeastern Spitsbergen, the remaining lower half of the Backluntdoppen Formation consists of variable proportions of similar facies and purely dolomitic grainstones and stromatolites. These heterogeneous facies give way in the middle Backlundtoppen Formation to a > 200 m-thick, monotonous interval of cliff-forming, dolomitic, club-shaped and branching columnar stromatolites, including *Baicalia*. This succession of stromatolites forms the regressive part of T-R5, the top of which marks an abrupt change to mixed siliciclastic and dolostone facies of the Kinnvika Member and thinner and better defined T-R sequences (Halverson et al., 2004).

The Kinnvika Member typically begins with a thin (10–20 m), shoaling-upward parasequence (T-R6a) consisting variably of siltstone or ribbon facies that transitions upward into microbialaminite (Fig. 5). In most sections, this parasequence is succeeded by a thicker (40–120 m) parasequence (T-R6b), the lower part of which is dominated by shale and grey to red siltstone to fine sandstone. These siliciclastic facies give way abruptly upward to the 1–25 m-thick "Dartboard dolomite" (cf. Wilson and Harland, 1964; Harland et al., 1993), which commonly is composed of lobate-cuspate laminations, in places oversteepened with up to 3 m of synoptic relief and concentric laminations in plan view, resembling *Conophyton* (Knoll et al., 1989). However, the Dartboard dolomite typically is heavily recrystallized and packed with isopachous cements, suggesting that the buckled laminations are more akin to typical supratidal tepee structures (Fig. 6a) than coniform stromatolites, although with some differences, as discussed further below.

In Nordaustlandet sections, the lower part of the Kinnvika Member contains scattered pinnacle reefs that grew vertically from the top of T-R6a and shed dolomite debris (coarse rudstone and floatstone) into this otherwise mainly siliciclastic interval (Halverson et al., 2004). The Dartboard dolomite in these sections commonly (but not universally) lacks the coniform structures, and it is instead distinguished by parallel laminated to undulose bedded dolostone, in places interbedded with microbialites, intraclast breccias or peloids (Halverson et al., 2004). Like the Spitsbergen sections, void-filling cements are common and the undulose bedding is in places cuspate; distinct from Spitsbergen sections, recrystallization is not pervasive and the cuspate structures are neither brecciated nor otherwise disrupted (Halverson et al., 2004). Subaqueous deposition is inferred, consistent with the nature of the contact of the overlying Russøya Member, as described below.

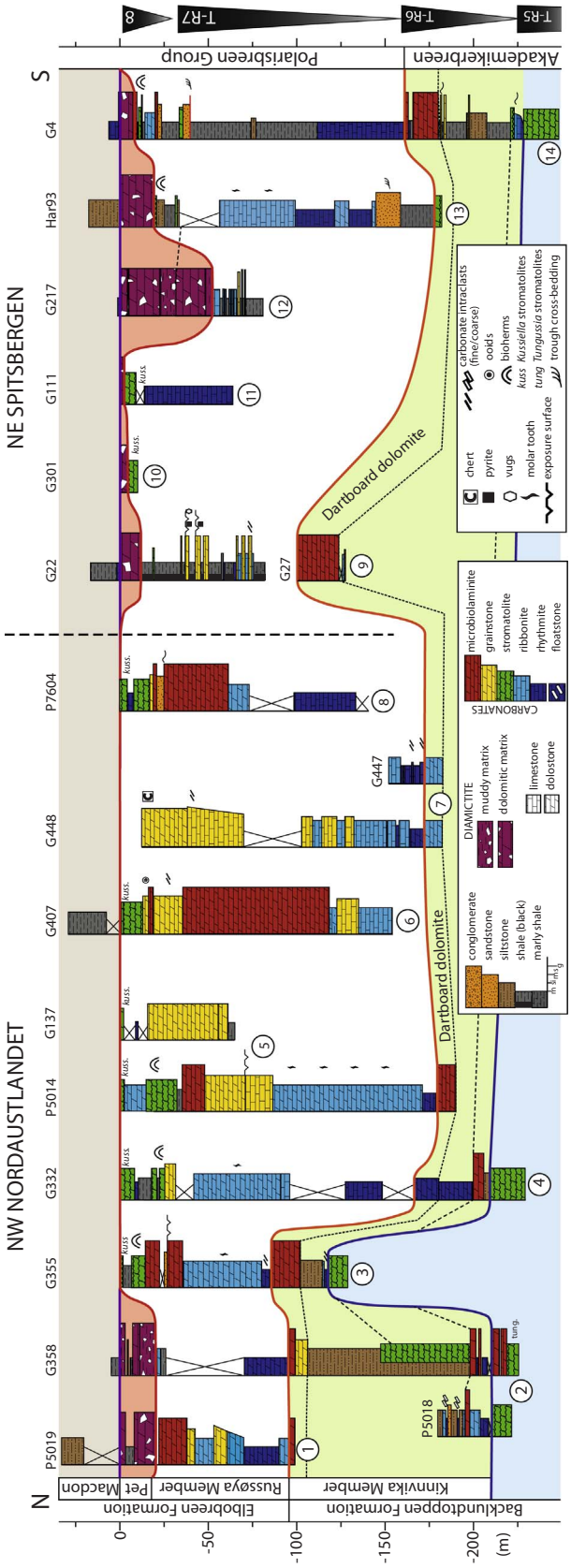

Fig. 5. Stratigraphic logs and correlations spanning the Kinnvika and Russøya members of the upper Backlundtoppen Formation (Akademikerbreen Group) and lower Elbobreen Formation (Polarisbreen Group). The 0 m datum is the contact between the Petrovbreen Member below (or Russøya Member where the Petrovbreen Member is absent) and the Macdonaldryggen Member above, chosen to illustrate inferred erosional truncation on the sub-glacial boundary (thick red line). Thick orange line shows correlation of the base of the Russøya Member (which is variably an exposure surface and a gradational boundary; Halverson et al., 2004). Fine dashed lines show correlations, including inferred onlap of the lowermost parasequence of the Kinnvika Member against what appears to be a paleotopographic high at this time at the location of section G355 on the north side of Murchisonfjord. Thick red line shows the sub-Petrovbreen unconformity, and thick purple line marks the contact between the Petrovbreen and Macdonaldryggen members. Sections G358, G355, G332, P5014, G137, G22, G111, G217, and G4 were previously published in Halverson et al. (2004), although section G4 here is modified based on more recent observations. Section Har93, logged by M. Hambrey and T.H. Jefferson, is reproduced from Harland et al. (1993). All other sections were previously unpublished. (For interpretation of the references to colour in this figure caption, the reader is referred to the web version of this article.)

3.3. Akademikerbreen-Polarisbreen contact

The top of the Kinnvika Member (i.e., Dartboard dolomite) marks the contact between the Akademikerbreen and Polarisbreen groups as currently defined (Wilson and Harland, 1964) (Fig. 5). In most Spitsbergen sections, the upper Dartboard dolomite is a heavily silicified solution breccia, with curved and tabular clasts lined by fringing cements and a muddy, silicified matrix that penetrates as much as 3 m downward from the contact. This breccia implies subaerial exposure, but no evidence for erosional truncation or deep karstification has been documented (Halverson et al., 2004).

In Nordaustlandet sections, this contact is commonly transitional rather than a sharp, brecciated surface. In these sections, the typically tan to yellow dolostone of the Dartboard dolomite grades into pink and tan, laminated dololutite and then into a finely laminated dolomitic marl and green shale, which marks the top of the transgressive systems tract of the overlying T-R sequence. In Spitsbergen sections, the lowermost Polarisbreen Group (the Russøya Member of the Elbobreen Formation) is poorly exposed.

3.4. The Polarisbreen Group

The Polarisbreen Group is subdivided into three formations (from bottom to top): the Elbobreen, Wilsonbreen, and Dracoisen formations (Hambrey, 1982). The Elbobreen Formation is in turn subdivided into four members, variably referred to (from bottom to top) as the Russøya, Petrovbreen, Macdonaldryggen, and Slangen members, or E1–4 (Fig. 2). The Petrovbreen Member and the Wilsonbreen Formation are distinct Cryogenian glacigenic units. Whereas Halverson et al. (2004) had proposed that the two units may have been deposited during a single glacial episode, the two units are now instead correlated confidently with the Sturtian and Marinoan glaciations, respectively (Hoffman et al., 2012).

The Russøya Member, discussed in more detail below, is a mixed siliciclastic-carbonate interval that spans T-R sequences 7 and 8. It varies in thickness from < 80 m to > 150 m and shows strong facies variations between the northern and southern parts of the outcrop belt, the former being more carbonate-rich and the latter more shaley. The upper Russøya Member preserves a large negative carbon isotope anomaly in carbonates ($\delta^{13}C_{carb}$) that is variably truncated in many sections by an erosional unconformity at the base of the overlying Petrovbreen Member marking the base of the early Cryogenian (Sturtian) glaciation in Svalbard.

The Petrovbreen Member varies from 0–52 m thick, but it is typically < 10 m thick and little more than a thin veneer in most Nordaustlandet sections (Hambrey, 1982; Harland et al., 1993; Halverson et al., 2004). Where present, it stands out as a yellow- to orange-weathering, poorly to massively stratified glaciomarine

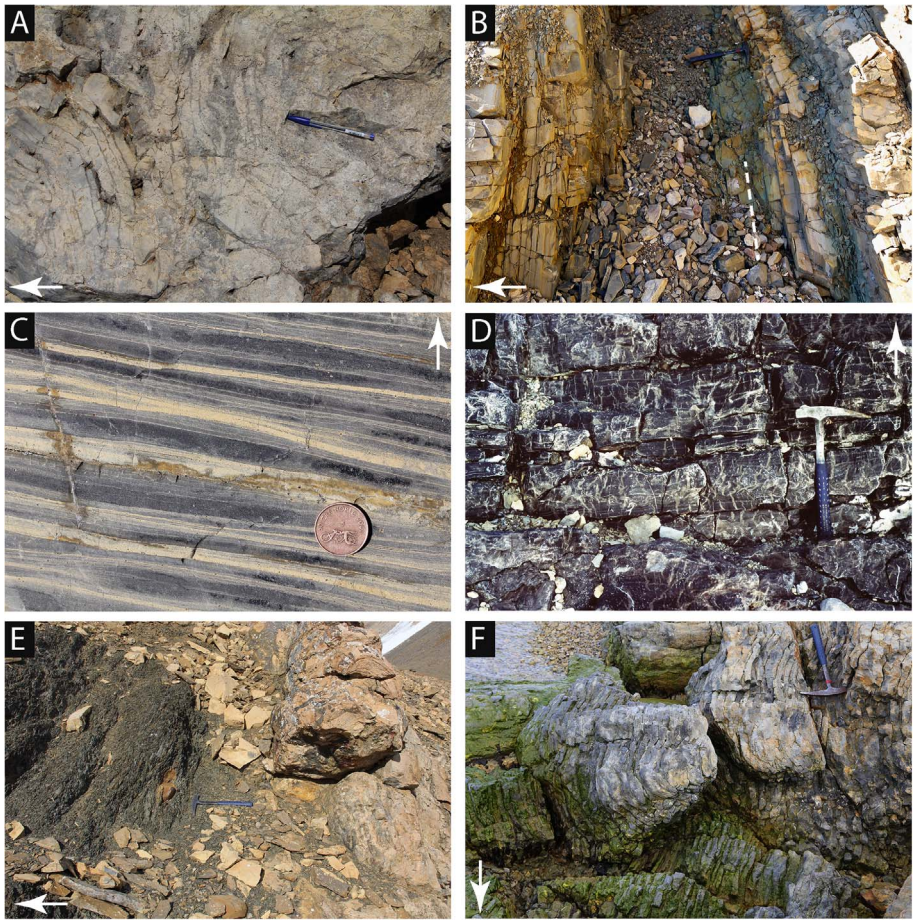

Fig. 6. Distinctive lithofacies in the upper Kinnvika and Russøya members. (A) Characterstically buckled and brecciated laminae and thin beds in the upper Dartboard dolomite in a typical section of the upper Kinnvika Member in northeastern Spitsbergen. (B) The transition between the upper Dartboard dolomite (to the right) and the lower Russøya Member to the left in a section where this contact is transitional rather than abrupt. Dashed line in green mudstone marks the maximum flooding surface of T-R7. (C) Typical laminated to thin-bedded, mixed black limestone and tan dolostone ribbon facies of the lower Russøya Member. (D) Intense molar tooth structure in the middle Russøya Member is one of the last extensive occurrence of this enigmatic sedimentary structure in the geological record (note hammer for scale near centre of photo). (E) Stromatolitic bioherms at the top of parasequence T-R8b in the upper Russøya Member, overlain by dark grey shale. Note the dolomitic concretion above the hammer head. (F) A biostrome of *Kussiella* stromatolites is the uppermost facies present in the Russøya Member, but it is commonly missing in Spitsbergen sections, where it is presumed to be truncated below the basal Petrovbreen Member glacial surface. White arrows show stratigraphic up in all photos. Hammer for scale is 33 cm long. Norwegian coin for scale in (C) is 19 mm in diameter.

diamictite and wackestone, with locally interbedded shales. Its clast composition is limited, comprising mainly sub-angular to angular black chert and dolomite derived from the underlying Russøya Member (Hambrey, 1982; Fairchild and Hambrey, 1984; Harland et al., 1993). The Petrovbreen Member is rarely overlain by a thin interval of very finely laminated, dark shaley limestone with variable, and in places highly depleted $\delta^{13}C_{carb}$ values (Halverson et al., 2004) suggesting a local authigenic origin that locally overprints the otherwise typical post-Sturtian values found in some sections (Fairchild et al., 2016a). In most sections the Petrovbreen Member is directly overlain by variably dolomitic shales and siltstone of the Macdonaldryggen Member. The Macdonaldryggen Member rarely is exposed in its entirety, but where it is, it is up to 215 m thick. It is distinguished by visible but subtle m-scale cyclicity (Fairchild et al., 2016a) and a lack of evidence for traction structures, implying deposition below storm wave base. It also shows evidence of syn-sedimentary slumping and folding and includes thin, pyritized laminae interpreted as the remnants of microbial mats (Fairchild et al., 2016a).

The upper Macdonaldryggen Member consists of limestone in some sections, recording the beginning of the shoaling-upward transition into the overlying Slangen Member, which consists of cross-bedded oolitic grainstones with interbedded fenestral microbialaminites and rare anhydrite (Fairchild and Hambrey, 1984; Halverson et al., 2004). Along with the underlying limestones of the upper Macdonaldryggen, the Slangen Member has exclusively positive $\delta^{13}C_{carb}$ signatures. In places, the contact with the overlying, glaciogenic Wilsonbreen Formation, is sharp, silicified, and brecciated. In more northerly sections, it is transitional through mud-cracked, dolomitic siltstone and up into sandstone of the Bråvika Member, which is made up of mostly pure quartz arenite with dolomitic rip-up clasts towards the base. The Bråvika Member is absent in all but the northernmost Spitsbergen sections but is everywhere present in Nordaustlandet, where it is transitional into the Wilsonbreen Formation and thickens to over 250 m in northernmost sections (Halverson et al., 2004).

The late Cryogenian (Marinoan) Wilsonbreen Formation reciprocates the thickness of the Bråvika Member and comprises a montage of terrestrial glacial and periglacial facies, recently described in detail by Fleming et al. (2016) and Fairchild et al. (2016b). The most distinct of these facies are carbonates, which include sulfate-rich limestones that preserve extremely negative triple oxygen isotope ($\Delta^{17}O$) anomalies (Bao et al., 2009). The Wilsonbreen Formation is overlain sharply by the Dracoisen Formation, the lowermost member of which is a typical basal Ediacaran cap dolostone, with distinctive megaripples, peloids, and $\delta^{13}C_{carb}$ values of -2 to -4‰ (Halverson et al., 2004). The cap dolostone is followed by calcareous red shales, then black-shales, and finally a thick succession of dominantly siltstone and fine sandstone with minor dolomite and anhydrite that records a transition to a restricted to non-marine environment (Fairchild and Hambrey, 1984). The upper contact of the Dracoisen is a major disconformity (Knoll and Swett, 1987), above which lie sandstones of the Lower Cambrian Tokammane Formation.

3.5. Age constraints

The Neoproterozoic strata in NE Svalbard have yet to be radiometrically dated; only a maximum age of ca. 940 Ma based on the age of rocks underlying the Veteranen Group in Nordaustlandet and detrital zircons (Johansson et al., 2000; Johansson et al., 2005; Aitken et al., 2017) can be directly applied to the succession. However, through correlation of the Cryogenian glacial deposits and the BSA with better dated counterparts on other continents, reliable ages can be imported and applied directly to the succession. A Re-Os age of 810 ± 5 m.y. on

organic-rich marl beneath the onset of the BSA in the Tatonduk inlier on the Yukon-Alaska border (Cohen et al., 2017) corroborates a U-Pb zircon chemical abrasion (CA) thermal ionization mass spectrometry (TIMS) age of 811.51 ± 0.25 Ma on a tuff located ~100 m beneath the onset of the BSA in the nearby Coal Creek inlier (central Ogilvie Mountains) of Yukon (Macdonald et al., 2010). Similarly, U-Pb zircon CA-TIMS ages of 815.29 ± 0.32 and 788.72 ± 0.24 Ma on tuffs below and above the end of the inferred BSA in the Tambien Group of Ethiopa (Swanson-Hysell et al., 2015) are consistent with dates from northwestern Canada. Swanson-Hysell et al. (2015) inferred that the BSA lasted between 7.3 and 16.9 m.y.

The age of the onset of the Sturtian glaciation in the Coal Creek inlier of Yukon (Canada) is tightly constrained to ca. 716.5 Ma by a series of precisely dated rhyolite flows and tuffs below and above the basal glacial surface (Macdonald et al., 2010, this volume). The contact between the Wilsonbreen and Dracoisen formations corresponds to the Cryogenian-Ediacaran boundary and is inferred to be ca. 635 Ma (Hoffmann et al., 2004; Condon et al., 2005; Calver et al., 2013). The top of the Dracoisen Formation is inferred to be > 580 Ma due to lack of evidence for Ediacaran fossils, the Shuram negative $\delta^{13}C$ anomaly, and Gaskiers glaciation (Halverson et al., 2004). Additional ages based on newly proposed correlations with northern Canada are discussed later in the text.

4. New data and data synthesis

In this paper we combine previously published and new stratigraphic and isotopic (carbonate and organic carbon and strontium) data from the upper Akademikerbreen and lower Polarisbreen groups to generate a stratigraphic and chemostratigraphic synthesis of the Tonian-Cryogenian transition in Svalbard. The complete data are then used to generate smoothed isotope profiles through this interval for better comparison with other successions and for use in compilations. The new and previously published data are included in Supplementary Table 1, and the smoothed data are presented in Supplementary Table 2.

4.1. Carbon and oxygen isotope ratios

Carbon ($\delta^{13}C_{carb}$) and oxygen ($\delta^{18}O_{carb}$) isotope ratios were analyzed in dual inlet mode on a Nu Perspective isotope ratio mass spectrometer connected to a NuCarb carbonate preparation system in the McGill University Stable Isotope Laboratory (Montréal, Canada). Approximately 80 µg of sample powder were weighed into glass vials and reacted individually with H_3PO_4 after heating to 90 °C for 1 h. The released CO_2 was collected cryogenically and isotope ratios were measured against an in-house reference gas in dual inlet mode. Samples were calibrated to VPDB (Vienna Pee Dee Belemnite) using in-house standards. Errors for both $\delta^{13}C_{carb}$ and $\delta^{18}O_{carb}$ were better than 0.05‰ (1σ) based on repeat analysis of standards.

All new carbon and oxygen isotope data (sections G447, G448, G523, GR16) are included in Supplementary Table 1, which also includes previously published $\delta^{13}C_{carb}$ and $\delta^{18}O_{carb}$ data (Halverson et al., 2004; Hoffman et al., 2012), organic carbon isotope ratios ($\delta^{13}C_{org}$; Halverson, 2011; Hoffman et al., 2012), and strontium isotope data (Halverson et al., 2007a; Cox et al., 2016) from these sections.

4.2. Smoothed $\delta^{13}C$ compilations

The stratigraphic heights corresponding to all available data from the Kinnvika and Russøya members were normalized to a single, composite stratigraphic column following correlations discussed below. A local regression smoothing technique (LOESS) was applied to both the $\delta^{13}C_{carb}$ and $\delta^{13}C_{org}$ data sets (Supplemental Table 2) to generate single curves with evenly spaced data points. The same technique was applied to the composite Svalbard Tonian section presented in Fig. 4 based on a compilation of previously published data.

5. Discussion

5.1. The late Tonian stratigraphic record in Svalbard

The contact between the Akademikerbreen and Polarisbreen groups broadly corresponds to a reorganization of the East Svalbard basin and a switch from dominantly carbonate to mixed carbonate-siliciclastic sedimentation. More specifically, the influx of siliciclastic sediments in the lower Kinnvika Member marks the end of a long-lived, highly stable carbonate platform. Although the top of the Backlundtoppen Formation below the Kinnvika Member (i.e., the contact between T-R5 and T-R6) is in places slightly brecciated, there is no evidence for subaerial exposure at this surface.

The Kinnvika Member typically begins with a thin (< 8 m) shoaling upward parasequence (T-R6a) comprising dolomitic shale or dololutite capped by orange microbialaminite. This parasequence is succeeded by an abrupt transgression, which in most parts of the outcrop belt is accompanied by a shift to green, red, and maroon shale and siltstone with minor mature, fine-grained quartz arenite beds. However, in sections near Bråvika (G358) and Gimleodden on Nordaustlandet (Fig. 1), this interval instead consists variably of stromatolite, stromatolitic breccia, and stromatolitic floatstone recording the growth of pinnacle reefs during this flooding event (Halverson et al., 2004). These pinnacle reefs attain a maximum measured thickness of 48 m and evidently provided a local source of carbonate sediments that include scattered intraclasts found within the bounding siliciclastic sediments. These reefs are found in the thickest Kinnvika sections.

No stromatolites are found in the correlative interval in Spitsbergen sections, but at Backlundtoppen (G4), a minor shoaling upward sequence (T-R6b) is capped by a thin bed of dolomitic grainstone. Here, this parasequence is followed by a third parasequence (T-R6c), which is capped by 14.3 m of the Dartboard dolomite, with the characteristic oversteepened and heavily cemented coniform microbialites. In Nordaustlandet, these two distinct parasequences in the middle and upper Kinnvika are not observed, and in one section (G355), the entire Kinnvika Member is a single parasequence that is only 30 m thick. This contrasts with section G358 some 10 km to the north where the Kinnvika Member has three distinct parasequences and is 125 m thick. The combination of the abrupt changes in thickness, influx of siliciclastic sediments, and rapid increase in local base level strongly suggests block rotation due to active extension early in Kinnvika Member times. The differential subsidence and local uplift partially segmented the basin, and rapid subsidence on down-dropped blocks resulted in flooding and growth of pinnacle reefs in T-R6b.

Although localized growth of pinnacle reefs helped to smooth the bathymetric relief on the seafloor following differential subsidence and uplift, significant relief persisted through deposition of the Dartboard dolomite. This relief is manifested in widely varying facies within the Dartboard dolomite, from the heavily cemented and warped microbialites common in most sections to persistently subaqueous stromatolites and ribbon facies in other locations (e.g. G447-448). The classic, heavily cemented Dartboard dolomite facies is interpreted to record subaerial exposure and intense evaporative pumping. The distinct aspect of this facies as compared to typical sabkha-type microbialaminite with tepee structures (e.g., Kendall and Warren, 1987) may be the result of regular (tidal or seasonal?) fluctuations between vadose and phreatic conditions and proximity to seawater. These hydrological conditions were presumably the consequence of the irregular bathymetry inherited from the local block rotation and subsidence during deposition of the lower Kinnvika Member.

In sections where the Dartboard dolomite is brecciated and heavily cemented, the contact with the overlying basal Russøya Member is sharp and disconformable and the transgressive systems tract (TST) of overlying T-R7 is thin or entirely absent. However, in sections not

characterized by the intense cementation, the contact is transitional and the TST is preserved, with dolomitic microbialites and dololutites passing upward into increasingly thinner bedded to laminated pink and tan dolostone, up to a distinct maximum flooding surface (MFS) marked by green dolomitic mudstone (Fig. 6b). The overlying regressive systems tract (RST) of T-R7 marks the base of the Russøya Member and typically consists of a combination of interbedded black limestone, silty dolostone, and shale with rare interbedded floatstone (Fig. 6c).

The Russøya Member can be subdivided into two T-R sequences (T-R7 and T-R8), each with constituent parasequences identified as higher order shoaling upward sequences. In northern sections, T-R7 is predominantly carbonate and is a well-defined shoaling upward sequence that typically begins with black shales and limestone rhythmites that grade upward into a thick interval of limestone ribbons with abundant black molar tooth structures (Fig. 6c), followed by limestone and dolomite grainstones with ooids, and finally microbialaminites that mark the sequence top. In contrast, although the lower Russøya Member in G4 consists of ~50 m of grey limestone rhythmites, southern sections are dominantly siliciclastic. Here, T-R7 is subdivided into two parasequences, the lower of which is variably capped by a siltstone and the upper of which comprises a shale capped by 4.5 m of red, trough cross-bedded quartz arenite. This arenite was likely deposited during a falling stage systems tract (FSST), implying that top of T-R7 represents a subaerial unconformity, which is consistent with brecciation and top truncation of a thin stromatolite unit that caps the parasequence in section G22 and the occurrence of microbialaminites at the top of the parasequence in Nordaustlandet sections (Fig. 7). The combination of a transition from platformal facies carbonates in the north part of the belt to dominantly shales with interbedded ferruginous dolostone beds in the south and the preservation of an FSST in the south suggests a north-to-south deepening, distally steepened carbonate platform at this time.

The upper Russøya Member above the basal T-R7 sequence is subdivided into three distinct parasequences (T-R8a-c) that can be correlated across the outcrop belt (Fig. 7). These parasequences are commonly mixed siliciclastic-carbonate, with basal shale overlain by carbonate. In section G4, T-R8a is capped by 2.5 m of red quartz arenite. Stromatolites occur variably in all three parasequences, but most commonly in the upper two. T-R8b includes grey columnar stromatolites, capped by distinct, m-scale bioherms (Fig. 6e), whereas TR-8c is distinguished by the occurrence of a biostrome of the columnar stromatolite *Kussiella*, which is up to 8.4 m thick and displays a distinctive corkscrew habit (Fig. 6f). In fact, the *Kussiella* biostrome is a useful marker bed and its presence or absence can be used to gauge the extent of erosional relief on the contact between the upper Russøya Member and the overlying Petrovbreen Member. Where the *Kussiella* biostrome is altogether absent, the Petrovbreen Member is thicker. In contrast, where the biostrome is present, the Petrovbreen Member is thin to absent (as in most Nordaustlandet sections). As described by Halverson et al. (2004), this relationship is part of a more general reciprocal pattern between the extent of erosion on the basal Petrovbreen disconformity and the thickness of the Petrovbreen Member, which is further elucidated by carbon isotope stratigraphy (Fig. 7) as discussed below.

5.2. Isotope chemostratigraphy

The Backlundtoppen Formation has among the highest $\delta^{13}C_{carb}$ values of the entire Neoproterozoic succession in Svalbard, exceeding 8‰ in the upper stromatolitic interval. However, this trend is interrupted by a downturn that corresponds precisely to the demise of the stable carbonate platform (Fig. 4). $\delta^{13}C_{carb}$ values begin to decline across the Backlundtoppen-Kinnvika contact, recover in stromatolites within the pinnacle reefs to values >6‰, and then decline again to values between 2–4‰ in the Dartboard dolomite.

The lower Russøya Member shows a distinct trend of increasing $\delta^{13}C_{carb}$, from values as low as ~ 0.5‰ to values >7‰ (Figs. 7, 10). This high in $\delta^{13}C_{carb}$ in the upper part of T-R7 is followed by a downturn to values near 0‰, then a recovery to mildly positive values. The beginning of the downturn towards the highly negative $\delta^{13}C_{carb}$ values of the

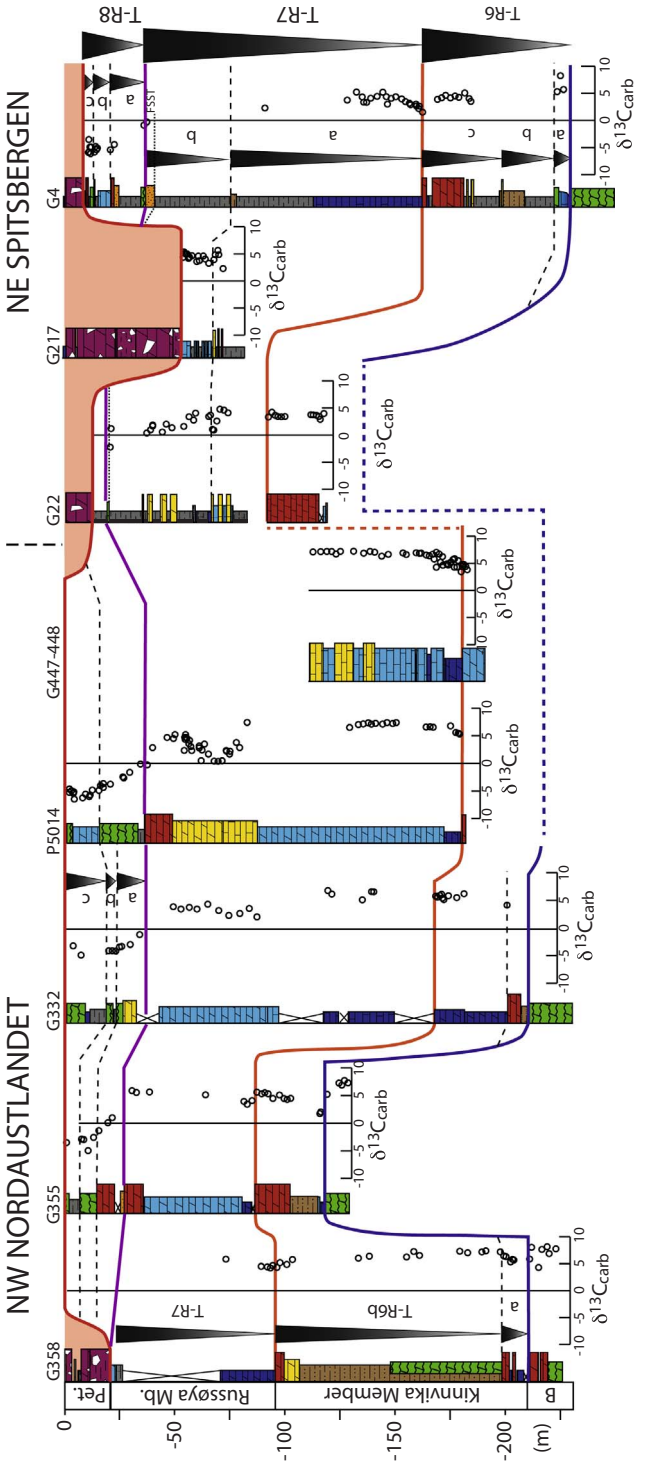

Fig. 7. Correlation of the parasequences of the Kinnvika and Russøya members and carbon isotope data for the subset of sections shown in Fig. 5 with available data. Thick unbroken lines are T-R sequence boundaries. Dashed lines are correlations of parasequence boundaries. Data from section G447-G448 is previously unpublished. A second set of data from the lower Russøya Member at Backlundtoppen is not plotted here, but is included in Supplementary Table 1. Note the preservation of a thin falling stage systems tract (FSST) in the uppermost T-R7 in section G4, which implies that the contact between T-R7 and T-R8 in more proximal sections is a subaerial exposure surface. Previously published data in other sections are from Halverson et al. (2004) and Hoffman et al. (2012). See Fig. 5 for legend.

carbon isotope anomaly in the upper Russøya Member coincides with the subaerial unconformity that marks the contact between T-R7 and T-R8 (Fig. 7). The minima of the anomaly and the beginning of a recovery towards slightly higher values occurs in T-R8c.

The upper Russøya negative $\delta^{13}C_{carb}$ anomaly is best preserved in the more carbonate-rich Nordaustlandet sections, but it is also found in section G4 in the southern part of the outcrop belt. That the anomalies in the carbonate-rich Nordaustlandet sections and mixed carbonate-siliciclastic Spitsbergen sections are one in the same is confirmed by the *Kussiella* biostrome, which everywhere has $\delta^{13}C_{carb}$ values between −2.5 and −4‰ that record a return to slightly less ^{13}C-depleted values following the $\delta^{13}C_{carb}$ minimum (Halverson et al., 2004). In two studied sections in Spitsbergen, G22 (Dracoisen) and G217 (Klufjellet), the full negative anomaly is missing and the *Kussiella* biostrome, along with the remainder of parasequence T-R8c, are missing. The absence of the anomaly and T-R8c is attributed to erosional truncation beneath the Petrovbreen Member (Halverson et al., 2004). This interpretation is consistent with correlation of the T-R8 parasequences across the outcrop belt and the occurrence of greater thickness of Petrovbreen Member diamictites in the truncated sections (Fig. 7).

The variable truncation of the pre-glacial anomaly in several sections and the evidence for a partial recovery towards less ^{13}C-depleted values in some sections (e.g., where the *Kussiella* biostrome is present) suggest that the Russøya negative anomaly was acquired syndepositionally and was not the result of meteoric diagenesis related to the subglacial surface. This inference is consistent with $\delta^{13}C_{org}$ values from the Russøya Member (from Halverson, 2011; Hoffman et al., 2012) that display a broadly similar pattern to the $^{13}C_{carb}$ values, including the negative anomaly in the upper Russøya Member, where $\delta^{13}C_{org}$ values drop as low as −32‰.

Only a handful of reliable strontium isotope data have been obtained from the Russøya Member (Halverson et al., 2007b; Cox et al., 2016), and none have been acquired on the Kinnvika Member, where the carbonate is exclusively dolomite. The available data (Supplementary Table 1) indicate effectively invariant $^{87}Sr/^{86}Sr$ ratios ~0.7067 throughout the Russøya Member.

5.3. Paleoredox data

Published paleoredox data from the Tonian stratigraphy in northeastern Svalbard include total organic carbon (TOC), iron speciation, Fe/Al ratios, redox-sensitive trace metals, multiple sulfur isotopes, and iron isotopes (Kunzmann et al., 2015, 2017a,b; Tahata et al., 2015). These data cover a wide stratigraphic range including the Oxfordbreen Formation of the upper Veteranen Group, the Svanbergfjellet and Backlundtoppen formations of the Akademikerbreen Group, and the Russøya Member of the Polarisbreen Group. However, more than half of the data come from the Russøya Member alone because in the Akademikerbreen and Veteranen groups, fine-grained, organic-rich silicilcastic rocks are mostly limited to maximum flooding intervals. Given the excellent preservation state of Akademikerbreen carbonates, however, future application of carbonate-hosted paleoredox proxies such as rare earth elements, I/Ca ratios, and non-traditional stable isotopes in carbonates (e.g., U isotopes) will likely shed more light onto the poorly understood redox chemistry of the Tonian ocean.

The previously analyzed Tonian samples were deposited under suboxic to anoxic-ferruginous conditions as implied by low TOC contents (most samples show a range from 0.5 to 1.5 wt%), iron speciation and Fe/Al data, and Mo, U, and V which show little authigenic enrichment (Kunzmann et al., 2015, Fig. 8). This interpretation is supported by bulk shale Fe isotope values which are significantly heavier than bulk continental crust and hydrothermal iron (Fig. 8), which is presumably the major iron source in mostly anoxic Precambrian marine environments. This enrichment in heavy isotopes implies non-quantitative oxidation of the ferrous seawater iron reservoir across the chemocline (Kunzmann et al., 2017b). Pyrite-specific Fe isotope data lead

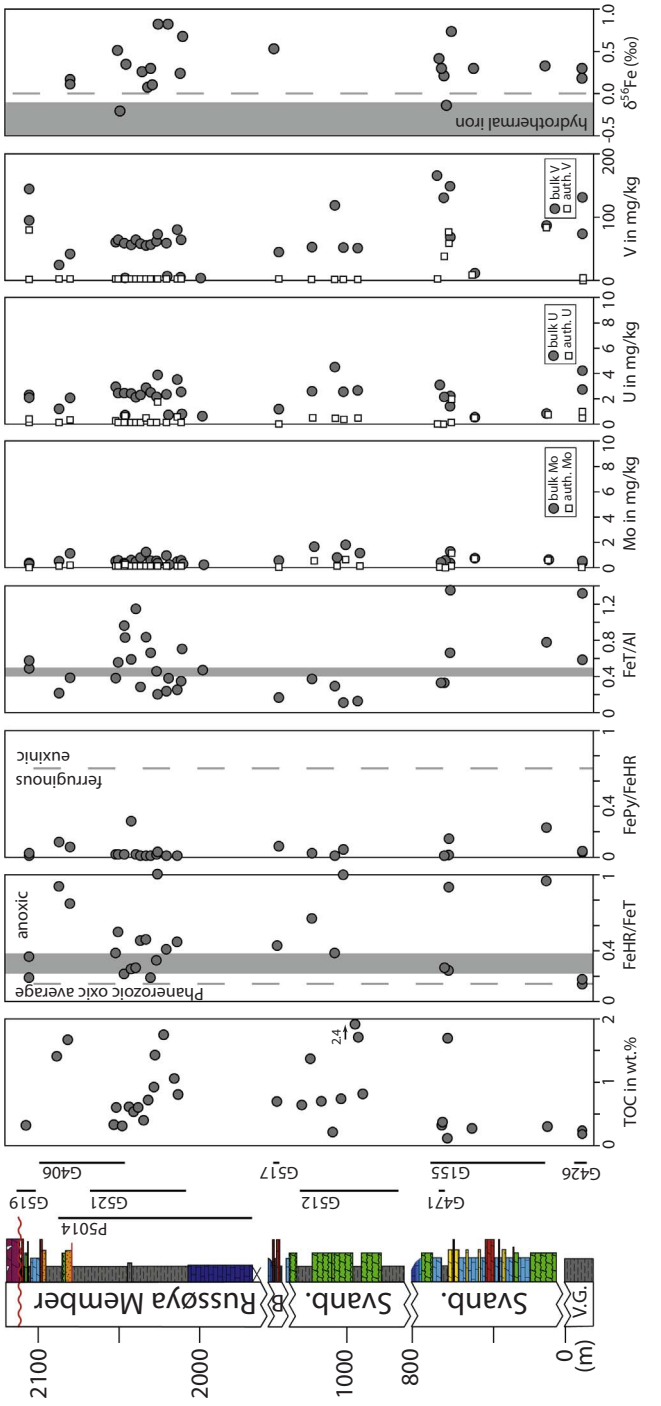

Fig. 8. Paleoredox data from the Tonian succession in northeastern Svalbard suggest deposition under dominantly suboxic to anoxic-ferruginous conditions (data from Kunzmann et al., 2015, 2017b). Vertical dashed line in the highly reactive iron/total iron (FeHR/FeT) plot represents the average of Phanerozoic oxic shales (Poulton et al., 2002). Shaded area in FeHR/FeT plot (0.22–0.38) marks equivocal results where samples may have been deposited under oxic or anoxic conditions (Poulton et al., 2011). Shaded area in the FeT/Al plot shows the composition of upper continental crust (UCC MacLennan, 2001). FeT/Al ratios higher than UCC indicate iron enrichment under anoxic conditions. Authigenic fractions in trace metal plots were calculated by subtracting the detrital fraction from the bulk rock concentration. The detrital fraction is calculated as: detrital trace metal = $(\text{trace metal/Al})_{UCC} \times Al_{sample}$ (cf. Kunzmann et al., 2015; Scott et al., 2017).

to the same conclusion because they show a large variation in $\delta^{56}Fe$ (Tahata et al., 2015). However, mineral-specific data should be treated with caution as pyrite formed under non-euxinic conditions may not

fully record seawater signals because it does not quantitatively capture dissolved ferrous iron (Berner, 1984).

A dominantly suboxic to anoxic-ferruginous water column during deposition of Tonian shales in northeastern Svalbard is consistent with the emerging view that anoxic-ferruginous conditions dominated the early Neoproterozoic ocean below storm wave base (Guilbaud et al., 2015; Sperling et al., 2015). Basin redox transects across the ca. 850–800 Ma Fifteenmile Group in northwestern Laurentia suggest that an oxic surface ocean overlay a dominantly anoxic-ferruginous deep ocean (Sperling et al., 2013). Ferruginous conditions also dominated the ca. 900–720 Ma Shaler Supergroup of the Amundsen Basin in northern Laurentia, with transient euxinic conditions occurring at the onset of the Bitter Springs Anomaly (Thomson et al., 2015b). Similarly, the > 742 Ma Chuar Group of the Grand Canyon Supergroup in Laurentia was deposited under a dominantly anoxic-ferruginous water column (Johansson et al., 2010).

An important question about ocean redox during the Tonian-Cryogenian transition is whether any change in environmental oxygen levels or in oceanic redox structure occurred leading into or spanning the Sturtian glaciation. This question is difficult to address because recent age constraints from Laurentia (Strauss et al., 2014; Rooney et al., 2014), combined with carbon isotope chemostratigraphy, indicate that a significant portion of the latest Tonian stratigraphic record was removed by the sub-Sturtian disconformity in most basins, including in East Svalbard (see discussion below). Available data, however, show no significant change in oceanic redox conditions across the Sturtian glaciation in the East Svalbard basin. Paleoredox data from the early Cryogenian Macdonaldryggen Member indicate continuation of dominantly anoxic-ferruginous conditions into the Cryogenian interglacial interval (Kunzmann et al., 2015; Tahata et al., 2015). A higher resolution study of the correlative Arena Formation in East Greenland in this volume identified an anoxic-sulfidic (euxinic) interval immediately overlying the Petrovbreen equivalent Ulvesø glacials (Scheller et al., this volume). This basal euxinic interval then transitions upward into shales deposited under anoxic-ferruginous conditions (Scheller et al., this volume). Additional evidence against significantly increasing environmental oxygen levels in the East Svalbard basin comes from multiple sulfur isotope data that span almost the entire Neoproterozoic succession in Svalbard. These data suggest that oxygen-driven re-organization of the marine sulfur cycle did not occur until the earliest Ediacaran (Kunzmann et al., 2017a).

Iron speciation and trace metal data from Cryogenian shales in the Nanhua Basin of South China (Li et al., 2012) and the Mackenzie Mountains in northwestern Canada (Sperling et al., 2016) similarly imply deposition under predominantly ferruginous conditions, with some oxic and euxinic intervals. Although these data confirm conclusions drawn from Svalbard that significant oxygenation did not occur across the Sturtian glaciation, Lau et al. (2017) recently argued for a period of increased oxygen levels in the Cryogenian ocean based on U isotopes in carbonates from the Taishir Formation in Mongolia. Notwithstanding the Mongolia data, the preponderance of redox data imply mainly anoxic and mainly ferruginous conditions prior to and following the Sturtian glaciation and through at least most of the Cryogenian interglacial interval.

5.4. Paleontology

The Hecla Hoek Series has proven to be a trove of microfossils and even macrofossils that have played a significant role in populating the Tonian biostratigraphic record. For example, the earliest unambiguous fossils of green and multicellular alga are found in the Svanbergfjellet Formation (Butterfield et al., 1988), which along with the overlying Draken Formation, preserves a diverse assemblage of sphaeromorphic acritarchs and cyanobacteria (Knoll et al., 1991; Butterfield et al., 1994). However, the Kinnvika and Russøya members are more notable for their paucity of fossils. The most significant fossils that occur in this interval are vase-shaped microfossils (VSMs), which are characteristic of the latest Tonian globally (Porter et al., 2003; Strauss et al., 2014). VSMs occur in intervals in the upper half of the Akademikerbreen Group, including the Kinnvika Member, and a single species (*C. torquata*) is found in chert nodules in the lower Russøya Member (Knoll, 1982; Porter et al., 2003; Rainbird and Porter, this volume).

5.5. Correlations of the upper Tonian of Svalbard with NW Laurentia

Halverson et al. (2004) initially correlated the upper Russøya negative $\delta^{13}C$ anomaly with the pre-Marinoan *Trezona* carbon isotope anomaly that is well documented in the Adelaide Rift-basin of South Australia (McKirdy et al., 2001; Rose et al., 2012), the Otavi Group of northern Namibia (Halverson et al., 2002), and the Mackenzie Mountains of northwestern Canada (Hoffman and Schrag, 2002; Halverson et al., 2005). This correlation implied that both the Petrovbreen Member and Wilsonbreen Formation, along with the intervening Macdonaldryggen and Slangen members (Fig. 2), were collectively deposited during the Marinoan glaciation. However, the combination of consistent $^{87}Sr/^{86}Sr$ values of 0.7067 throughout the Russøya Member, contrasting with ratios > 0.7071 in the upper Cryogenian interglacial interval in Mongolia, Namibia, and elsewhere (Halverson et al., 2007b; Bold et al., 2016), and documentation of a pre-Sturtian negative carbon isotope anomaly in Scotland (Prave et al., 2009) and northwestern Laurentia (Halverson, 2006) rendered this hypothesis improbable (Hoffman et al., 2012). Instead it appears that negative carbon isotope anomalies occur prior to both the Sturtian and Marionan glaciations, but that the latter (Trezona) anomaly is missing in Svalbard (Hoffman et al., 2012).

The late Tonian carbonate chemostratigraphic record is well-documented in northwestern Canada. The Coates Lake Group of the Mackenzie Mountains, which sits between the Little Dal Group below and the early Cryogenian Rapitan Group above, preserves a prominent negative carbon isotope anomaly in the Coppercap Formation, with values as low as −6‰ that are superseded by a smooth recovery to highly positive values (Fig. 9; Halverson, 2006; Rooney et al., 2014). A Re-Os age of 732.2 ± 3.9 Ma on organic-rich carbonates dates the crossover back to positive values during this recovery (Rooney et al., 2014).

In the Ogilvie Mountains in Yukon, where the onset of Cryogenian glaciation is precisely dated to ca. 716.5 Ma by U-Pb ID-TIMS geochronology (Macdonald et al., 2010; Macdonald et al., this volume), the Mount Harper Group occupies a similar stratigraphic position to the Coates Lake Group. The lower, dominantly carbonate Callison Lake Formation forms the base of the Mount Harper Group, and in the Mount Harper region of Yukon (Coal Creek inlier), it is overlain by conglomerates of the Seela Pass Formation and the mainly basaltic Mount Harper Volcanics (Strauss et al., 2015). The upper Callison Lake Formation records a reproducible negative carbon isotope anomaly, and its correlation with the Coppercap anomaly is supported by a Re-Os age of 739.9 ± 6.1 Ma from just below the isotopic minimum (Strauss et al., 2014; Strauss et al., 2015). Another Re-Os age of 752.7 ± 5.5 Ma from the lower Callison Lake Formation (Strauss et al., 2014) helps to calibrate the carbon isotopic record preceding the onset of the Coppercap negative $\delta^{13}C$ anomaly (Fig. 9).

The Kilian Formation in the upper Shaler Supergroup of Victoria Island occupies an analogous stratigraphic position to the Callison Lake Formation and Coates Lake Group and similarly preserves a negative $\delta^{13}C$ anomaly that occurs well before the onset of Sturtian glaciation (Fig. 9; Jones et al., 2010; Thomson et al., 2015b). Strauss et al. (2015) identified three unconformity-bound transgressive-regressive sequences (T-R6, T-R7, T-R8) in the Callison Lake Formation and correlated these with the Coates Lake Group (again comprising three T-R sequences) and three similar sequences in the Kilian Formation (Rainbird, 1993; Thomson et al., 2015a). In all three regions, the lowermost of these sequences marks a significant unconformity and/or change in style in

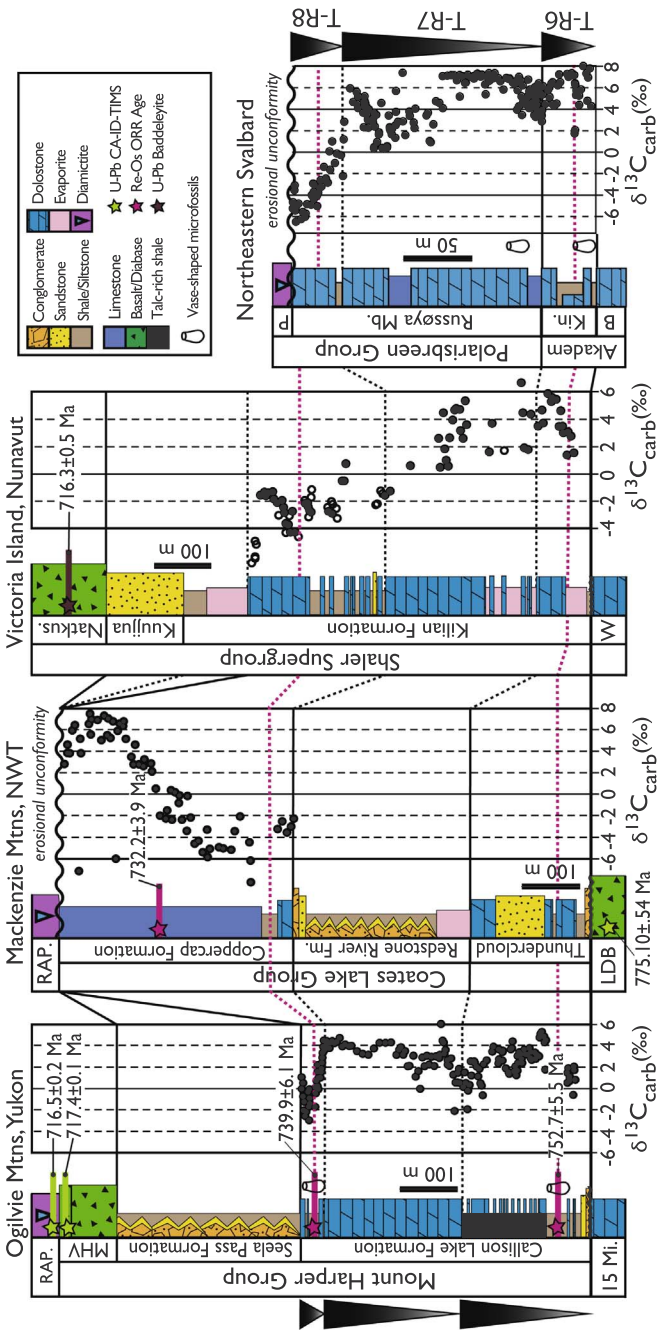

Fig. 9. Proposed correlations between the upper Tonian strata of Svalbard (Kinnvika and Russøya members) and pre-Cryogenian successions in northwestern Canada. Dashed pink lines show inferred correlations of horizons dated by Re-Os geochronology. 15 Mi = Fifteenmile Group; LDB = LIttle Dal Basalt; W = Wynniatt Formation; B = Backlundtoppen Formation. U-Pb ages from Macdonald et al. (2010, 2017). Re-Os ages from Strauss et al. (2014) and Rooney et al. (2014). T-R sequences (inverted shaded triangles) as in Fig. 7. Modified from Strauss et al. (2015).

sedimentation. For example, the contact between the Callison Lake Formation and the underlying Fifteenmile Group is variably an angular unconformity or significant disconformity (Macdonald and Roots, 2010; Strauss et al., 2015), as is the contact between the basal Coates Lake Group and the underlying ca. 775 Ma Little Dal Basalt (Milton et al., 2017), which caps the Little Dal Group in the Mackenzie Mountains (Aitken, 1982). In both cases, these latest Tonian sedimentary packages record renewed extension and subsidence that initiated the Windermere depositional cycle in the Canadian Cordillera. These basins were superimposed upon long-lived early Neoproterozoic intracratonic basins whose origin significantly preceded the development of the latest Proterozoic–Paleozoic Cordilleran passive margin.

The three T-R sequences in the Callison Lake Formation and the encompassed carbon isotope profile correlate remarkably well and in detail with the three T-R sequences that comprise the Kinnvika and Russøya members (Fig. 9). Similarly, vase-shape microfossils, occur at the base of T-R8 in both the Callison Lake Formation and the equivalent sequence in the lower Russøya Formation (Fig. 9; Strauss et al., 2014; Rainbird and Porter, this volume). Analogous to northwestern Canada, the basal Kinnvika Member records a major reorganization of the East Svalbard basin. These late Tonian successions in northern Laurentia also correlate with the ChUMP basins of the southwestern United States: the late Tonian Chuar Group in the Grand Canyon region of Arizona, the Uinta Mountain Group of Utah, and the Middle Pahrump Group of the Death Valley Region (Strauss et al., 2014; Dehler et al., 2017). These units all preserve similar negative carbon isotope anomalies in organic carbon or carbonate as the Callison Lake Formation, contain VSMs and record local extension near the future continental margin of Laurentia (Dehler et al., 2017; Strauss et al., 2014; Smith et al., 2016). Hence, it appears that a broad arc of the Laurentian margin—at least from the southwest to the northeast—experienced incipient continental extension in the late Tonian as a prelude to eventual disintegration of Rodinia.

5.6. Calibrating the late Tonian record in East Svalbard and implications for the Tonian-Cryogenian transition

Accepting these correlations, we can apply the Re-Os ages from the Callison Lake Group directly to the East Svalbard Succession. The 752.7 ± 5.5 Ma date in the lowermost T-R sequence in the lower Callison Lake Formation correlates with T-R6b in the Kinnvika Member, and the 739.9 ± 6.1 Ma age from the uppermost T-R sequence in the upper Callison Lake Formation occurs just below the $\delta^{13}C_{carb}$ minima, and hence correlates to near the boundary between T-R8a and T-R8b in the upper Russøya Member. This correlation implies that a significant amount of time is missing on the disconformable contact between the Russøya and Petrovbreen members. It follows that the recovery from this negative anomaly back to highly ^{13}C-enriched values, as recorded in the Coppercap Formation, where it is constrained to be >732.2 ± 3.9 Ga, is missing in Svalbard (Fig. 9). An analogous recovery from a late Tonian negative carbon isotope anomaly occurs in the Tambien Group of Namibia (Swanson-Hysell et al., 2015) and Bed-group 20 in East Greenland (Fairchild et al., 2000; Klaebe et al., this volume). Accepting the ca. 716.5 Ma age for the onset of Sturtian glaciation in Svalbard, between ca. 13.5 m.y. and 29.5 m.y. of the stratigraphic record at the transition from the Tonian to Cryogenian periods is absent in even the most complete sections of the Russøya Member. Therefore, even though the relief developed on the sub-Petrovbreen disconformity is relatively small (< 50 m), either this relief represents only a fraction of the total strata removed, the ca. 13.5–29.5 m.y. immediately preceding the onset of Cryogenian glaciation was an interval of non-deposition, or both factors combined to account for the missing end Tonian record.

Despite the implication that the Polarisbreen Group does not provide a complete record of the Tonian-Cryogenian transition, data from the Kinnvika and Russøya members nevertheless provide important information for documenting the transition between these two periods. The carbon isotope record from Svalbard leading up to the upper Russøya anomaly is one of the most complete for this poorly studied interval in late Tonian Earth history and is now reasonably well calibrated based on Re-Os ages from northwestern Canada (Fig. 10). This same interval preserves some of the latest significant occurrence of molar tooth structures (Fig. 6d) in Earth's history; possibly slightly younger molar tooth structures occur in Bed-groups 19 and 20 of the upper Eleonore Bay Group, East Greenland (Fairchild et al., 2000), but no significant occurrences are known to post-date the onset of the

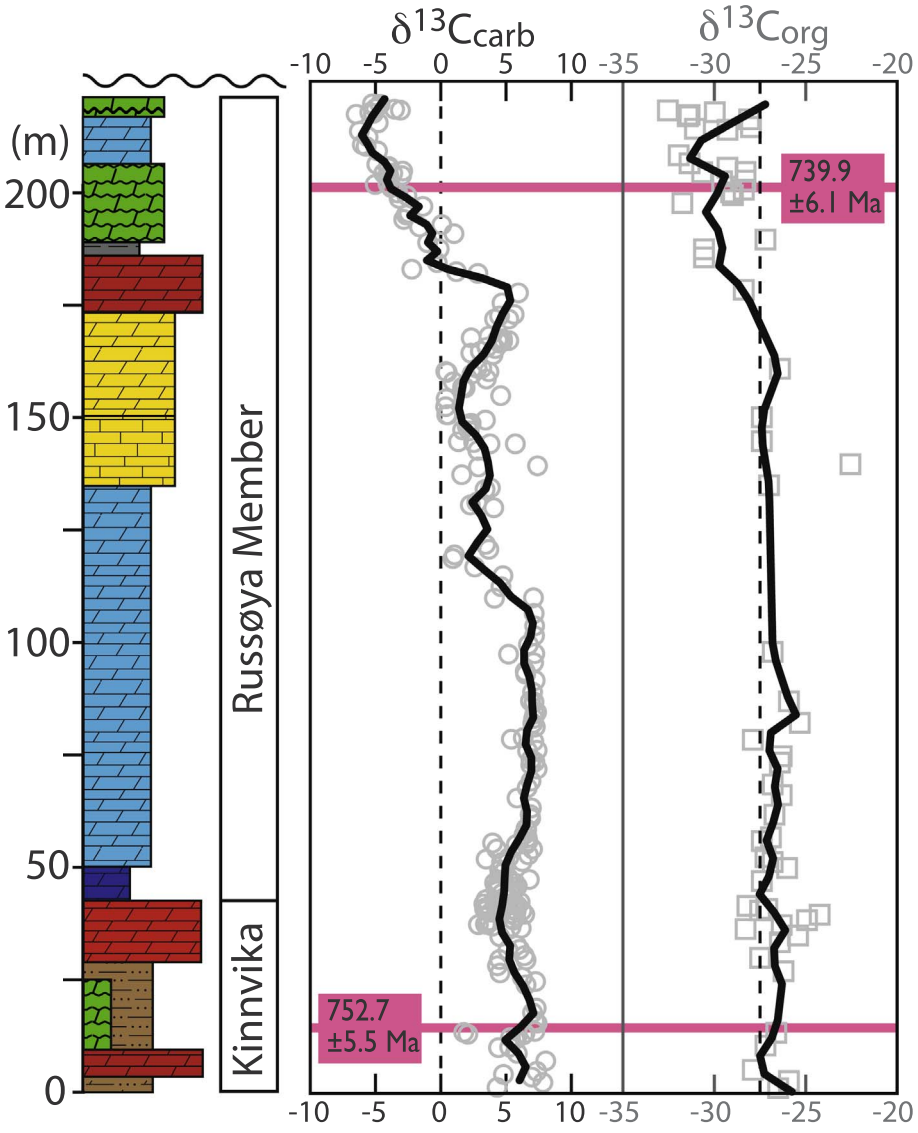

Fig. 10. Composite stratigraphic profile and carbonate and organic carbon $\delta^{13}C$ data for the combined Russøya and Kinnvika members, along with ages derived from correlation with the Callison Lake Formation in Yukon, Canada. Circles represent all available data, and solid black lines are LOESS fits of these data, which are provided in tabular form in Supplementary Table 2.

Cryogenian period (Shields-Zhou et al., 2016; Hodgskiss et al., 2018).

Strontium isotope data from the Russøya Member establish that seawater $^{87}Sr/^{86}Sr$ was ~0.7067 ca. 750–740 Ma, prior to the end Russøya negative $\delta^{13}C_{carb}$ anomaly. Bed-group 19 in East Greenland preserves a negative carbon isotope anomaly of a similar magnitude and in an analogous stratigraphic position to the upper Russøya anomaly, but in slope facies (Fairchild et al., 2000; Klaebe et al., this volume). The overlying Bed-group 20, which records a return to highly positive $\delta^{13}C_{carb}$ values in shallow-water carbonate facies, has $^{87}Sr/^{86}Sr$ values near 0.7063 (Fairchild et al., 2000). The lowest $\delta^{13}C_{carb}$ values in Bed-group 19 are lower than any recorded in Svalbard, and the carbon isotope trends in Bed-groups 19 and 20 have been interpreted to record the effect depth gradients in $\delta^{13}C$ (Fairchild et al., 2000), possibly related to a depth-dependent influence on authigenic carbonate content, rather a change in seawater compositions (Klaebe et al., this volume). However, given that the Russøya anomaly is preserved in shallow water carbonates at the same stratigraphic interval in the same basin (Fig. 1 in Klaebe et al., this volume), the depth-dependence hypothesis cannot explain these anomalies. Hence, we interpret the Russøya and Bed-group 19 anomalies to be equivalent anomalies recording a primary seawater signal in inner platform (Nordaustlandet), distal platform (Spitsbergen), and slope (East Greenland) environments. The return to positive values occurred during a subsequent drop in base level (i.e., Bed-group 20), accounting for its absence in Svalbard. In other words Bed-group 20 represents the continuation of the T-R8 sequence, which was only preserved in the deeper part of the basin where sedimentation continued during the forced regression. The absence of the return to positive values and Bed-group 20 on Ella Ø in East Greenland is likely the result of erosional removal, consistent with evidence for a sharp erosional contact with the overlying Ulvesø Formation in East Greenland (Stouge et al., 2011; Hoffman et al., 2012).

The correlation between the Russøya and Bed-group 19 anomalies implies that $^{87}Sr/^{86}Sr$ of seawater dropped during the recovery from the upper Russøya anomaly and prior to the onset of Cryogenian glaciation. This conclusions supports the correlation between the upper Russøya and Coppercap $\delta^{13}C_{carb}$ anomalies (Fig. 9), because the return to positive $\delta^{13}C_{carb}$ in the latter is also associated with a downturn in $^{87}Sr/^{86}Sr$ (Rooney et al., 2014; Cox et al., 2016).

Another place where a late Tonian negative carbon isotope anomaly occurs is in the Appin Group (Dalradian Supergroup) of Scotland (Prave et al., 2009; Sawaki et al., 2010). The *Islay anomaly* as initially reported is similar in magnitude and shape to the upper Russøya anomaly and also shows the onset of a return to positive values just beneath the contact with the overlying glaciogenic Port Askaig Formation. However, Fairchild et al. (this volume) revisited the stratigraphic context and reproducibility of this anomaly and found that a primary negative $\delta^{13}C_{carb}$ anomaly does not occur on Islay, but rather that the pre-glacial anomaly is confined to the newly defined Garb Eileach Formation, as

recorded in the Garvellach Islands. Nevertheless, the rebranded *Garvellach anomaly* has a similar shape and strontium isotope signature (0.7064–0.7066 Fairchild et al., this volume) to the upper Russøya Member anomaly. Unlike the upper Russøya Member, the Garb Eileach Formation appears to transition into overlying glacial deposits without a stratigraphic break (Fairchild et al., this volume). Assuming a globally synchronous ca. 717 Ma onset to Sturtian glaciation (Rooney et al., 2015), this important difference implies an age of ca. 720–717 Ma for the Garb Eileach anomaly, which is some 20 m.y. younger than the age inferred for the Russøya anomaly based on correlations with northern Laurentia (Fig. 10).

The conundrum posed by the apparently very different ages for the Coppercap anomaly and the Garvellach anomaly has three possible solutions. First, the proposed ages for either the Garb Eileach or Coppercap anomalies are incorrect, which would allow these and the Russøya anomaly all to be equivalent. Second, some or all of the anomalies may be secondary (i.e., diagenetic) or local signatures that do not represent global perturbations to the seawater DIC reservoir. Third, there may be two distinct negative carbon isotope anomalies with similar strontium isotope signatures during the late Tonian, but separated in time by as much as 20 million years. Lacking any other justification at this time for dismissing the proposed ages, which are consistent with a growing body of data in support of globally synchronous onset and demise of the Cryogenian glaciations, we consider the first option unlikely. The second option is plausible, but is also unlikely given that in northern Canada, the Coppercap anomaly is preserved in the same stratigraphic context in multiple different basins and sections within each basin, and in Svalbard, the Russøya anomaly is preserved in detail in multiple different, carbonate-rich sections.

If we accept the third explanation of two distinct anomalies, then either (1) the Russøya anomaly does not correlate with the Coppercap anomaly but does correlate with the younger Garvellach anomaly or (2) the Russøya anomaly does correlate with the Coppercap anomaly as proposed in Fig. 9, but neither northern Canada nor Svalbard preserves the younger, Garvellach anomaly. Because the stratigraphic record in Svalbard lacks any evidence for a significant stratigraphic discontinuity between the Bitter Springs Anomaly and the Russøya anomaly, it seems unlikely that the record of another anomaly is simply missing in these rocks. Hence, the simplest interpretation and one that we explore here is that the Garvellach anomaly represents a second, end-Tonian, negative carbon isotope anomaly that is up to 20 m.y. younger than the Coppercap-Russøya anomaly but missing in northern Laurentia below the sub-Sturtian erosional unconformity.

In the Dalradian Supergroup, a second, older late Tonian negative $\delta^{13}C_{carb}$ anomaly occurs in the Ballachulish Limestone, middle Appin Group, beneath the Garvellach anomaly (Prave et al., 2009). This anomaly was originally correlated with the BSA (Prave et al., 2009), but the magnitude of the anomaly is much greater (−7‰) than is characteristic of the BSA (Halverson et al., 2007b), and subsequent authors have suggested that it is younger than the BSA (Rooney et al., 2011; Fairchild et al., this volume). A post-BSA age for the Ballachulish anomaly is also more consistent with strontium isotope data. No primary strontium isotope data exist for the Ballachulish Limestone, but the anomaly is bracketed by $^{87}Sr/^{86}Sr \approx 0.7065$ below and $^{87}Sr/^{86}Sr \approx 7.070$ above (Thomas et al., 2004; Fairchild et al., this volume). These data are in the same range as $^{87}Sr/^{86}Sr$ data for the Coppercap Formation and Russøya Member (Halverson et al., 2007a; Rooney et al., 2014), but distinctly more radiogenic than the BSA, with $^{87}Sr/^{86}Sr \approx 0.7063$ (Halverson et al., 2007b).

Swanson-Hysell et al. (2015) previously suggested that an earlier, well-defined negative $\delta^{13}C_{carb}$ anomaly (formerly referred to as the Islay anomaly), preceded a second downturn to negative $\delta^{13}C_{carb}$ values leading into Sturtian glaciation. This inference was based on integration of new U-Pb ages and carbon isotope data from the Tambien Group of Ethiopia with other calibrated $\delta^{13}C_{carb}$ compilations for the Tonian period. If the Garvellach anomaly also records this younger anomaly, the Garb Eileach Formation may provide an even more complete record of $\delta^{13}C_{carb}$ prior to Sturtian glaciation, with a distinct upturn towards less ^{13}C-depleted values, as seen also in the pre-Marinoan Trezona anomaly (Halverson et al., 2002; Rose et al., 2012). The possibility of a pair of the late Tonian (ca. 740–717 Ma) negative carbon isotope anomalies is provocative in light of attempts to link the carbon isotope record to mechanisms for the onset of Sturtian glaciation (e.g. Cox et al., 2016). If the late Tonian ocean did in fact suffer two deep negative carbon isotope anomalies, why is the second so poorly represented in most Tonian-Cryogenian sections globally? One possibility is that the contact beneath Sturtian glacial deposits tends to be a significant disconformity or even angular unconformity due to the combined effects of deep eustatic sea level fall and active rifting in many Sturtian-aged basins globally (Cox et al., 2013). Consequently, only fortuitously situated sections may preserve the end-Tonian Garvellach anomaly, and for these sections, there is no guarantee that they will also preserve the older Coppercap-Russøya anomaly.

6. Conclusions

The Eastern Province of northeastern Svalbard boasts one of the best preserved and most complete middle to late Tonian sections in the world. It is also the source of a wealth of geochemical, micropaleontological, and sedimentological data that inform the study of Neoproterozoic paleoenvironments. Inasmuch, the Akademikerbreen and Polarisbreen groups of the upper Hecla Hoek Series serve as a valuable reference section for middle Neoproterozoic time. In order to contribute to the discussion about the eventual placement of the basal Cryogenian GSSP, as well as debates about Neoproterozoic oxygenation and the trigger mechanisms for the onset of Cryogenian glaciation, we have presented here a synthesis of lithostratigraphic, sequence stratigraphic, chemostratigraphic and redox data spanning the transition interval from the Tonian to the Cryogenian in East Svalbard.

These data and resulting interpretation yield important implications for the evolution and paleogeography of the East Svalbard basin, global paleoenvironmental change prior to the onset of Cryogenian glaciation, and the completeness of the latest Tonian stratigraphic record. The base of the Kinnvika Member marks the demise of a long-lived, stable tropical carbonate platform recorded by the Akademikerbreen Group (and the quivalent Ymer Ø and Andrée Land groups in East Greenland). This demise was likely the result of extension and fault block rotation giving rise to differential uplift and subsidence. Activity on these faults likely continued through at least the middle Russøya Member and probably accounted for significant facies variations between carbonate-dominated northern sections (i.e. Nordaustlandet) and siliciclastic-dominated southern sections of the Russøya Member. The continuation of this southward-deepening (in current Svalbard coordinates) carbonate ramp is seen in Bed-group 19 of East Greenland, which represents a slope environment. Multiple redox proxy data from the Russøya Member imply a sub-oxic to anoxic ferruginous water column in this basin, consistent with limited data from this interval in other basins (Kunzmann et al., 2015; Kunzmann et al., 2017b).

The Russøya Member preserves a coherent, regionally reproducible carbon isotope record that includes at its top a well-defined, deep, negative carbon isotope anomaly. Correlations aided by sequence stratigraphy and carbon isotope chemostratigraphy suggest that the Kinnvika and Russøya members approximately correlate with the Callison Lake Formation, Coates Lake Group, and Killian Formation of northwestern to north-central Laurentia, the former two of which were deposited following renewed extension prior to the emplacement of the Franklin LIP and onset of Cryogenian glaciation (Strauss et al., 2015). This correlation implies an age of ca. 740 Ma for the Russøya anomaly and a significant erosional unconformity or depositional hiatus between the top of the Russøya Formation and the overlying glaciogenic Petrovbreen Member. However, the return to positive carbon isotope values is recorded in Bed-group 20 of East Greenland (Fairchild et al.,

2000; Klaebe et al., this volume), which was likely deposited during an interval of base level fall that entirely post-dates the Russøya Member.

The Russøya anomaly had previously been correlated with the so-called Islay anomaly in Scotland (e.g., Halverson and Shields-Zhou, 2011; Hoffman et al., 2012) that occurs beneath the Port Askaig Tillite Formation in Scotland (e.g., Sawaki et al., 2010). However, Fairchild et al. (this volume) revisit the stratigraphic framework for this anomaly and conclude that it is only found reliably in the Garb Eileach Formation of the Garvellach Islands. Furthermore, the Garb Eileach Formation appears to be transitional into the glaciogenic Port Askaig Formation (Fairchild et al., this volume). Insofar as the onset of early Cryogenian (Sturtian) glaciation is globally synchronous at ca. 717 Ma (Rooney et al., 2014; Rooney et al., 2015), then if the proposed age for the Russøya anomaly is broadly correct, it cannot correlate with the newly named *Garvellach anomaly*. The implication is that there may have been two distinct, global negative carbon isotope anomalies during the late Tonian of similar magnitude, separated by up ca. 20 m.y. This hypothesis implies that the Russøya Formation is significantly top-truncated, such that East Svalbard, like many other regions globally, is missing the latest Tonian stratigraphic record.

The poor accessibility of the Neoproterozoic strata of northeast Svalbard, along with the lack of any direct radiometric ages and the significant hiatus beneath the Petrovbreen glacial deposits, make the Polarisbreen Group poorly suited for defining the basal Cryogenian GSSP. However, the Akademikerbreen Group below boasts continuous stratigraphic coverage, mostly in little altered carbonate, spanning the ca. 810–800 Ma Bitter Springs negative carbon isotope anomaly. With the large revision to the lower limit of the Cryogenian period, the Tonian period has expanded to about 280 m.y. in duration. After the Cryogenian period is formalized and attention shifts to revising and formally defining the Tonian period, northeastern Svalbard will be a logical starting point for discussion.

Acknowledgments

Early fieldwork in Svalbard (1999–2002) by GPH and ACM was supported NASA Astrobiology and NSF grants to Paul F. Hoffman. GPH acknowledges funding from the Natural Sciences and Engineering Research Council (NSERC) Discovery program, which financed his most recent fieldwork in Svalbard. MK publishes with permission of the executive director of the Northern Territory Geological Survey. JVS acknowledges support from the Department of Earth Sciences at Dartmouth College and NSF Tectonics Division (EAR-1650152). This manuscript greatly benefited from new and renewed observations made during fieldwork with K. Bergmann, N. Tosca, and T. Mackey in 2016 and was significantly improved by detailed comments by Ian Fairchild and an anonymous reviewer.

Appendix A. Supplementary data

Supplementary data associated with this article can be found, in the online version, at http://dx.doi.org/10.1016/j.precamres.2017.12.010.

References

Aitken, J.D., 1982. Precambrian of the Mackenzie fold belt–a stratigraphic and tectonic overview. In: Hutchison, R.W., Spence, C.D., Franklin, J.M. (Eds.), Precambrian Sulfide Deposits, H.S. Robinson Memorial Volume, Special Paper 25. Geological Association of Canada, St. John's, pp. 149–161.

Allen, T.J., Cornish Morales, I.M., Wallace, V.C., Pipejohn, K., Bergmann, K., Halverson, G.P., Tosca, N.J., McClelland, W.C., Strauss, J.V., 2017. Detrital zircon geochronology and provenance of the Hecla Hoek Succession of northeastern Svalbard, Norway. In: Geological Society of America Annual Meeting Abstracts with Programs. Vol. 49. pp. 1–.1130/abs/2017AM–294506.

Bao, H., Fairchild, I.J., Wynn, P.M., Spötl, C., 2009. Stretching the envelope of past surface environments: Neoproterzoic glacial lakes from Svalbard. Science 323, 119–122.

Benn, D.I., Le Hir, G., Bao, H., Donnadieu, Y., Dumas, C., Fleming, E.J., Hambrey, M.J., McMillan, E.A., Petronis, M.S., Ramstein, G., Stevenson, C.T.E., Wynn, P.M., Fairchild, I.J., 2015. Orbitally forced ice sheet fluctuations during the Marinoan Snowball Earth glaciation. Nat. Geosci. 8, 704–707.

Berner, R.A., 1984. Sedimenatry pyrite formation: an update. Geochimica et Cosmochemica Acta 48, 605–615.

Bjørnerud, M.G., 2010. Stratigraphic record of Neoproterozoic ice sheet collapse: the Kapp Lyell diamictite sequence, SW Spitsbergen, Svalbard. Geol. Mag. 147, 380–390.

Bold, U., Smith, E.F., Rooney, A.D., Bowring, S.A., Buchwald, R., Dudas, F.O., Rameani, J., Crowley, J.L., Schrag, D.P., Macdonald, F.A., 2016. Neoproterozoic stratigraphy of the Zavkhan Terrane of Montolia: the backbone for Cryogenian and early Ediacaran chemostratigraphic records. Am. J. Sci. 316, 1–63.

Butterfield, N.J., Knoll, A.H., Swett, K., 1988. Exceptional preservation of fossils in an Upper Proterozoic shale. Nature 334, 424–427.

Butterfield, N.J., Knoll, A.H., Swett, K., 1994. Paleobiology of the Neoproterozoic Svanbergfjellet Formation, Spitsbergen. Fossils Strata 1–81.

Calver, C.R., Crowley, J.L., Wingate, M.T.D., Evans, D.A.D., Raub, T.D., Schmitz, M.D., 2013. Globally synchronous Marinoan deglaciation indicated by U-Pb geochronology of the Cottons Breccia, Tasmania, Australia. Geology 41, 1127–1130.

Cawood, P.A., Strachan, R., Cutts, K., Kinny, P.D., Hand, M., Pisarevsky, S., 2010. Neoproterozoic orogeny along the margin of Rodinia: Valhalla orogen, North Atlantic. Geology 38, 99–102.

Cawood, P.A., Strachan, R.A., Pisarevsky, S.A., Gladkochub, D.P., Murphy, J.B., 2016. Linking collisional and accretionary orogens during Rodinia assembly and breakup: implications for models of supercontinent cycles. Earth Planet. Sci. Lett. 449, 118–126.

Cohen, P.A., Strauss, J.V., Rooney, A.D., Sharma, M., Tosca, N., 2017. Controlled hydroxyapatite biomineralization in an ~810 million year old unicellular eukaryote. Sci. Adv. 3, e1700095.

Condon, D., Zhu, M., Bowring, S., Jin, Y., Wang, W., Yang, A., 2005. From the Marinoan glaciation to the oldest bilaterians: U-Pb ages from the Doushantuo Formation, China. Science 308, 95–98.

Cox, G.M., Halverson, G.P., Minarik, W.G., Le Heron, D.P., Macdonald, F.A., Bellefroid, E.J., Strauss, J.V., 2013. Neoproterozoic iron formation: an evaluation of its temporal, environmental and tectonic significance. Chem. Geol. 362, 232–249.

Cox, G.M., Halverson, G.P., Stevenson, R.K., Vokaty, M., Poirier, A., Kunzmann, M., Li, Z.-X., Denyszyn, S.W., Strauss, J.V., Macdonald, F.A., 2016. Continental flood basalt weathering as a trigger for Neoproterozoic Snowball Earth. Earth Planet. Sci. Lett. 446, 89–99.

Dallmann, W., Elvevold, S., 2013. Geoogical Map Svalbard, 1:200,000, sheet de45g, noraustlandet sw. Tech. Rep.. Norsk Polarinstitutt.

Dehler, C., Gehrels, G., Porter, S., Heizler, M., Karlstrom, K., Cox, G., Crossey, L., 2017. Synthesis of the 780–740 Ma Chuar, Uinta Mountain, and Pahrump (ChUMP) groups, western USA: implications for Laurentia-wide cratonic marine basins. Geol. Soc. Am. Bull. 129, 607–624.

Fairchild, I., Hambrey, M., 1995. Vendian basin evolution in East Greenland and NE Svalbard. Precambrian Res. 73, 217–333.

Fairchild, I.J., Bonnand, P., Davies, T., Fleming, E.J., Grassineau, N., Halverson, G.P., Hambrey, M.J., McMillan, E.M., McKay, E., Parkinson, I.J., Stevenson, C.T.E., 2016a. The Late Cryogenian Warm Interval, NE Svalbard: chemostratigraphy and genesis. Precambrian Res. 281, 128–154.

Fairchild, I.J., Fleming, E.J., Bao, H., Benn, D.I., Boomer, I., Dublyansky, Y.V., Halverson, G.P., Hambrey, M.J., Hendy, C., McMillan, E.A., Spötl, C., Stevenson, C.T.E., Wynn, P., 2016b. Continental carbonate facies of a Neoproterozoic panglaciation, north-east Svalbard. Sedimentology 63, 443–497.

Fairchild, I.J., Hambrey, M.J., 1984. The Vendian succession of northeastern Spitsbergen: petrogenesis of a dolomite-tillite association. Precambrian Res. 26, 111–167.

Fairchild, I.J., Knoll, A.H., Swett, K., 1993. Coastal lithofacies and biofacies associated with syndepositional dolomitization and silicification (Draken Formation, Upper Riphean, Svalbard). Precambrian Res. 53, 165–197.

Fairchild, I.J., Spencer, T., Ali, D., Anderson, R., Anderton, R., Boomer, I., Dove, D., Evans, J., Hambrey, M., Howe, J., Sawaki, Y., Wang, Z., Shields, G., Zhou, Y., Skelton, A., Tucker, M., this volume. Tonian-Cryogenian boundary sections of Argyll, Scotland. Precambrian Research.

Fairchild, I.J., Spiro, B., Herrington, P.M., Song, T., 2000. Controls on Sr and C isotope compositions of Neoproterozoic Sr-rich limestones of East Greenland and North China. In: Grotzinger, J., James, N. (Eds.), Carbonate Sedimentation and Diagenesis in an Evolving Precambrian World: SEPM Special Publication 67. SEPM, pp. 297–313.

Fleming, E.J., Benn, D.I., Stevenson, C.T.E., Petronis, M.S., Hambrey, M.J., Fairchild, I.J., 2016. Glacitectonism, subglacial and glacilacustrine processes during a Neoproterozoic panglaciation, north-east Svalbard. Sedimentology 63, 411–442.

Flood, B., Gee, D.G., Hjelle, A., Siggerud, T., Winsnes, T., 1969. The geology of Nordaustlandet, northern and central parts. Norsk Polarinstitutt Skrifter 146, 1–139.

Gasser, D., Andresen, A., 2013. Caledonian terrane amalgamation of Svalbard: detrital zircon provenance of Mesoproterozoic to Carboniferous strata from Oscar II Land, western Spitsbergen. Geol. Mag. 150, 1103–1126.

Gee, D.G., Tebenkov, A.M., 1996. Two major unconformities beneath the Neoproterozoic Murchisonfjorden Supergroup in the Caledonides of central Nordaustlandet, Svalbard. Polar Res. 15, 81–91.

Gee, D.G., Teben'kov, A.M., 2004. Svalbard: a fragment of the Laurentian margin. In: The Neoproterozoic Timaride Orogen of Eastern Baltica. Vol. 30 of Memoirs. Geological Society, London, pp. 191–206.

Gee, E.G., Page, L.M., 1994. Caledonian terrane assembly on Svalbard: new evidence from $^{40}Ar/^{39}Ar$ dating in Ny Friesland. Am. J. Sci. 294, 1166–1186.

Guilbaud, R., Poulton, S.W., Butterfield, N.J., Zhu, M., Shields-Zhou, G.A., 2015. A global transition to ferruginous conditions in the early Neoproterozoic oceans. Nat. Geosci. 8, 466–470.

Halverson, G.P., 2006. A neoproterozoic chronology. In: Xiao, S., Kaufman, A. (Eds.), Neoproterozoic Geobiology and Paleobiology. Vol. 27 of Topics in Geobiology. Springer, Dordrecht, the Netherlands, pp. 231–271.
Halverson, G.P., 2011. Glacial sediments and associated strata of the Polarisbreen Group, northeastern Svalbard. In: Arnaud, E., Halverson, G.P., Shields-Zhou, G. (Eds.), The Geological Record of Neoproterozoic Glaciations, Memoir 36. The Geological Society, London, pp. 571–579.
Halverson, G.P., Dudas, F.O., Maloof, A.C., Bowring, S.A., 2007a. Evolution of the $^{87}Sr/^{86}Sr$ composition of Neoproterozoic seawater. Palaeogeogr., Palaeoclimatol., Palaeoecol. 256, 103–129.
Halverson, G.P., Hoffman, P.F., Schrag, D.P., Kaufman, A.J., 2002. A major perturbation of the carbon cycle before the Ghaub glaciation (Neoproterozoic) in Namibia: prelude to snowball Earth? Geochem., Geophys., Geosyst. 3. http://dx.doi.org/10.1029/2001GC000244.
Halverson, G.P., Hoffman, P.F., Schrag, D.P., Maloof, A.C., Rice, A.H., 2005. Towards a Neoproterozoic composite carbon isotope record. Geol. Soc. Am. Bull. 117, 1181–1207.
Halverson, G.P., Maloof, A.C., Hoffman, P.F., 2004. The Marinoan glaciation (Neoproterozoic) in northeast Svalbard. Basin Res. 16, 297–324.
Halverson, G.P., Maloof, A.C., Schrag, D.P., Dudas, F.O., Hurtgen, M.T., 2007b. Stratigraphy and geochemistry of a ca 800 Ma negative carbon isotope interval in northeastern Svalbard. Chem. Geol. 237, 5–27.
Halverson, G.P., Shields-Zhou, G., 2011. Chemostratigraphy and the Neoproterozoic glaciations. In: Arnaud, E., Halverson, G.P., Shields-Zhou, G. (Eds.), The Geological Record of Neoproterozoic Glaciations. Memoir 36. Geological Society of London, London, pp. 51–66.
Hambrey, M., 1982. Late Precambrian diamictites of northeastern Svalbard. Geol. Mag. 127 527–515.
Harland, W., 1964. Critical evidence for a great infra-Cambrian glaciation. Geologisches Rundschau 54, 45–61.
Harland, W., Gayer, R., 1972. The Arctic Caledonides and earlier Oceans. Geol. Mag. 426, 289–384.
Harland, W.B., Hambrey, M.J., Waddams, P., 1993. Vendian Geology of Svalbard: Skrifter 193. Norsk Polarinstitutt, Oslo.
Harland, W.B., Scott, R.A., Auckland, K.A., Snape, I., 1992. The Ny Friesland Orogen, Spitsbergen. Geol. Mag. 129, 679–708.
Harland, W.B., Wilson, C.B., 1956. The Hecla Hoek succession in Ny Friesland, Spitsbergen. Geol. Mag. 93, 265–286.
Harland, W.B., Wright, N.J.R., 1979. Alternative hypothesis for the pre-Carboniferous evolution of Svalbard. Norsk Polarinstitutt Skrifter 167, 89–117.
Hodgskiss, M.S.W., Kunzmann, M., Poirier, A., Halverson, G.P., 2018. The role of microbial iron reduction in the formation of Proterozoic molar tooth structures. Earth Planet. Sci. Lett. 482, 1–11.
Hoffman, P.F., Halverson, G.P., Domack, E.W., Maloof, A.C., Swanson-Hysell, N.L., Cox, G.M., 2012. Cryogenian glaciations on the southern tropical paleomargin of Laurentia (NE Svalbard and East Greenland), and a primary origin for the upper Russøya (Islay) carbon isotope excursion. Precambrian Res. 206–207, 137–158.
Hoffman, P.F., Schrag, D.P., 2002. The snowball Earth hypothesis: testing the limits of global change. Terra Nova 14, 129–155.
Hoffmann, K.H., Condon, D.J., Bowring, S.A., Crowley, J.L., 2004. A U-Pb zircon date from the Neoproterozoic Ghaub Formation, Namibia: constraints on Marinoan glaciation. Geology 32 (9), 817–820.
Johansson, A., Gee, D.G., Larionov, A.N., Ohta, Y., Tebenkov, A.M., 2005. Grenvillian and Caledonian evolution of eastern Svalbard—a tale of two orogenies. Terra Nova 17, 317–325.
Johansson, A., Larianov, A.N., Tebenkov, A.M., Gee, D.G., Whitehouse, M.J., Vestin, J., 2000. Grenvillian magmatism of western and central Nordaustlandet, northeastern Svalbard. Trans. R. Soc. Edinburgh 90, 221–234.
Johnston, D.T., Poulton, S.W., Dehler, C., Porter, S., Husson, J., Canfield, D.E., Knoll, A.H., 2010. An emerging picture of Neoproterozoic ocean chemistry: Insights from the Chuar Group, Grand Canyon, USA. Earth Planet. Sci. Lett. 290, 64–73.
Jones, D.S., Maloof, A.C., Hurtgen, M.T., Rainbird, R.H., Schrag, D.P., 2010. Regional and global chemostratigraphic correlation of the early Neoproterozoic Shaler Supergroup, Victoria Island, Northwestern Canada. Precambrian Res. 181, 43–63.
Kaufman, A.J., Knoll, A.H., Narbonne, G.M., 1997. Isotopes, ice ages, and terminal Proterozoic Earth history. Proc. Nat. Acad. Sci. 95, 6600–6605.
Kendall, C.S.C., Warren, J., 1987. A review of the origin and setting of tepees and tehir associated fabrics. Sedimentology 34, 1007–1027.
Klaebe, R., Smith, P., Fairchild, I., Fleming, E., Kennedy, M., this volume. Basin evolution and the onset of the Sturtian Glaciation in NE Greenland. Precambrian Research.
Knoll, A., Swett, K., 1990. Carbonate deposition during the late Proterozoic Era: an example from Spitsbergen. Am. J. Sci. 290-A, 104–132.
Knoll, A.H., 1982. Microfossil-based biostratiraphy of the Precambrian Hecla Hoek sequence, Nordaustlandet, Svalbard. Geol. Mag. 119, 269–279.
Knoll, A.H., Hayes, J.M., Kaufman, A.J., Swett, K., Lambert, I.B., 1986. Secular variation in carbon isotope ratios from Upper Proterozoic successions of Svalbard and east Greenland. Nature 321, 832–837.
Knoll, A.H., Swett, K., 1987. Micropaleontology across the Precambrian-Cambrian boundary in Spitsbergen. J. Paleontol. 61, 898–926.
Knoll, A.H., Swett, K., Burkhart, E., 1989. Paleoenvironmental distribution of microfossils and stromatolites in the Upper Proterozoic Backlundtoppen Formation, Spitsbergen. J. Paleontol. 63, 129–145.
Knoll, A.H., Swett, K., Mark, J., 1991. Paleobiology of a Neoproterozoic tidal flat/lagoonal complex: the Draken Conglomerate Formation, Spitsbergen. J. Paleontol. 65, 531–570.
Kunzmann, M., Bui, T.H., Crockford, P.W., Halverson, G.P., Scott, C., Lyons, T.W., Wing, B.A., 2017a. Bacterial sulfur disproportionation constrains timing of Neoproterozoic oxygenation. Geology 45 (3), 207–210.
Kunzmann, M., Gibson, T.M., Halverson, G.P., Hodgskiss, M.S.W., Bui, T.H., Carozza, D.A., Sperling, E.A., Poirier, A., Cox, G.M., Wing, B.A., 2017b. Iron isotope biogeochemistry of Neoproterozoic marine shales. Geochim. Cosmochim. Acta 209, 85–105.
Kunzmann, M., Halverson, G.P., Scott, C.T., Minarik, W.G., Wing, B.A., 2015. Geochemistry of Neoproterozoic black shales from Svalbard: implications for oceanic redox conditions spanning Cryogenian glaciations. Chem. Geol. 417, 383–393.
Lau, K.V., Macdonald, F.A., Maher, K., Payne, J.L., 2017. Uranium isotope evidence for temporary ocean oxygenation in the aftermath of the Sturtian Snowball Earth. Earth Planet. Sci. Lett. 458, 282–292.
Li, C., Love, G.D., Lyons, T.W., Scott, C.T., Feng, L., Huang, J., Chang, H., Zhang, Q., Chu, X., 2012. Evidence for a redox stratified Cryogenian marine basin, Datangpo Formation, South China. Earth Planet. Sci. Lett. 331–332, 246–256.
Li, Z.-X., Evans, D.A.D., Halverson, G.P., 2013. Neoproterozoic glaciations in a revised global palaeogeography from the breakup of Rodinia to the assembly of Gondwanaland. Sed. Geol. 294, 219–232.
Macdonald, F.A., Roots, C.F., 2010. Upper Fifteenmile Group in the Ogilvie Mountains and correlations of early Neoproterozoic strata in the northern Cordillera. In: McFarlane, K.E., Weston, L.H., Blackburn, L.R. (Eds.), Yukon Exploration and Geology 2009. Yukon Geological Survey, pp. 237–252.
Macdonald, F.A., Schmitz, M.D., Crowley, J.L., Roots, C.F., Jones, D.S., Maloof, A.C., Strauss, J.V., Cohen, P.A., Johnston, D.T., Schrag, D.P., 2010. Calibrating the Cryogenian. Science 327, 1241–1243.
Macdonald, F.A., Schmitz, M.D., Strauss, J., Halverson, G.P., Gibson, T., Eyster, A., Cox, G., Mamrol, P., Crowley, J., this volume. The Cryogenian of Yukon. Precambrian Res.
Macdonald, F.A., Wordsworth, R., 2017. Initiation of Snowball Earth with volcanic sulfur aerosol emissions. J. Geophys. Res. 44, 1938–1946.
MacLennan, S.M., 2001. Relationships between the trace element composition of sedimenatry rocks and upper continental crust. Geochem., Geophys., Geosyst. 2 Paper number 2000GC000109.
Majka, J., Be'eri-Shlevin, Y., Gee, D.G., Czerny, J., Frei, D., Ladenberger, A., 2014. Torellian (c. 640 Ma) metamorphic overprint of Tonian (c. 950 Ma) basement in the Caledonides of southwestern Svalbard. Geol. Mag. 151, 732–748.
Maloof, A.C., Halverson, G.P., Kirschvink, J.L., Schrag, D.P., Weiss, B., Hoffman, P.F., 2006. Combined paleomagnetic, isotopic and stratigraphic evidence for true polar wander from the Neoproterozoic Akademikerbreen Group, Svalbard. Geol. Soc. Am. Bull. 118, 1099–1124.
Mazur, S., Czerny, J., Majka, J., Manecki, M., Holm, D., Smyrak, A., Wypych, A., 2009. A strike-slip terrane boundary in Wedel Jarlsberg Land, Svalbard, and its bearing on correlations of SW Spitsbergen with the Pearya terrane and Timanide belt. J. Geol. Soc. 166 (529–544), 529–544.
McKirdy, D.M., Burgess, J.M., Lemon, N.M., Yu, X., Cooper, A.M., Gostin, V.A., Jenkins, R.J.F., Both, R.A., 2001. A chemostratigraphic overview of the late Cryogenian interglacial sequence in the Adelaide Fold-Thrust Belt, South Australia. Precambrian Res. 106, 149–186.
Milton, J.E., Hickey, K.A., Gleeson, S.A., Friedman, R.M., 2017. New U-Pb constraints on the age of the Little Dal Basalts and Gunbarrel-related volcanism in Rodinia. Precambrian Res. 296, 168–180.
Ohta, Y., 1994. Caledonian and Precambrian history in Svalbard: a review, and an implication of escape tectonics. Tectonophysics 231, 183–194.
Ohta, Y., Dallmeyer, R.D., Peucat, J.J., 1989. Caledonian terranes in Svalbard. In: Dallmeyer, R.D. (Ed.), Terranes in the Circum Atlantic Paleozoic Orogens 230. Geological Society of America Special Publication, pp. 1–15.
Pettersson, C.H., Pease, V., Frei, D., 2009. U-Pb zircon provenance of metasedimentary basement of the Northwestern Terrane, Svalbard: implications for the Grenvillian-Sveconorwegian orogeny and development of Rodinia. Precambrian Res. 175, 206–220.
Porter, S.A., Meisterfield, R., Knoll, A.H., 2003. Vase-shaped microfossils from the Neoproterozoic Chuar Group, Grand Canyon: a classification guided by modern testate amoebae. J. Paleontol. 77, 409–429.
Poulton, S.W., Canfield, D.E., 2011. Ferruginous conditions: a dominant feature of the ocean through Earth's history. Elements 7, 107–112.
Poulton, S.W., Raiswell, R., 2002. The low-temperature geochemical cycle of iron: from continental fluxes to marine sediment deposition. Am. J. Sci. 302, 774–805.
Prave, A.R., Fallick, A.E., Thomas, C.W., Graham, C.M., 2009. A composite C-isotope profile for the Neoproterozoic of Scotland and Ireland. J. Geol. Soc., London 166, 845–857.
Rainbird, R.H., 1993. The sedimentary record of mantle plume uplift preceding eruption of the Neoproterozoic Natkusiak flood basalt. J. Geol. 101, 305–318.
Riedman, L.A., Porter, S.A., this volume. Vase-shaped microfossil biostratigraphy with new data from Tasmania, Svalbard, Greenland, Sweden and the Yukon. Precambrian Res.
Rooney, A.D., Chew, D.M., Selbey, D., 2011. Re–Os geochronology of the Neoproterozoic-Cambrian Dalradian Supergroup of Scotland and Ireland: Implications for Neoproterozoic stratigraphy, glaciations and Re–Os systematics. Precambrian Res. 185, 202–214.
Rooney, A.D., Macdonald, F.A., Strauss, J.V., Dudás, F.O., Hallmann, C., Selby, D., 2014. Re-Os geochronology and coupled Os-Sr isotope constraints on the Sturtian snowball Earth. Proc. Nat. Acad. Sci. 111, 51–56.
Rooney, A.D., Strauss, J.V., Brandon, A.D., Macdonald, F.A., 2015. A Cryogenian chronology: two long-lasting synchronous Neoproterozoic glaciations. Geology 43, 459–462.
Rose, C.V., Swanson-Hysell, N.L., Husson, J.M., Poppic, L.N., Cottle, J.M., Schoene, B., Maloof, A.C., 2012. Constraints on the origin and relative timing of the Trezona $\delta^{13}C$

anomaly below the end-Cryogenian glaciation. Earth Planet. Sci. Lett. 319–320, 241–250.
Sandelin, S., Tebenkov, A.M., Gee, D.G., 2001. The stratigraphy of the lower part of the Neoproterozoic Murchisonfjorden Supergroup in Nordaustlandet, Svalbard. GFF 123, 113–127.
Sawaki, Y., Kawai, T., Shibuya, T., Tahata, M., Omori, S., Komiya, T., Yoshida, N., Hirata, T., Ohno, T., Windley, B.F., Maruyama, S., 2010. $^{87}Sr/^{86}Sr$ chemostratigraphy of Neoproterozoic Dalradian carbonates below the Port Askaig glaciogenic Formation, Scotland. Precambrian Res. 179, 150–164.
Scheller, E.L., Dickson, A.J., Canfield, D.E., Korte, C., Kristiansen, K.K., Dahl, T.W., this volume. Ocean redox conditions between the Snowballs – geochemical constraints from the Arena Formation, East Greenland. Precambrian Res.
Scott, C., Slack, J.F., Kelley, K.D., 2017. The hyper-enrichment of V and Zn in black shales of the Late Devonian Early Mississppian Bakken Formation (USA). Chem. Geol. 452, 24–33.
Shields-Zhou, G., Porter, S.A., Halverson, G.P., 2016. A new rock-based definition for the Cryogenian Period (circa 720-635 Ma). Episodes 39, 3–8.
Smith, E.F., Macdonald, F.A., Crowley, J.L., Hodgin, E.B., Schrag, D.P., 2016. Tectonostratigraphic evolution of the c. 780-730 Ma Beck Spring Dolomite: Basin Formation in the core of Rodinia. In: Li, Z.X., Evans, D.A.D., Murphy, J.B. (Eds.), Supercontinent Cycles Through Earth History, vol. 424. Geological Society of London, pp. 213–239.
Sperling, E.A., Carbone, C., Johnston, D.T., Narbonne, G.M., Macdonald, F.A., 2016. Oxygen, time and facies controls on the appearance of the Cryogenian and Ediacaran body and trace fossils in the Mackenzie Mountains, Northwest Territories, Canada. Geol. Soc. Am. Bull. 128 (3–4), 558–575.
Sperling, E.A., Halverson, G.P., Knoll, A.H., Macdonald, F.A., Johnston, D.T., 2013. A basin redox transect at the dawn of animal life. Earth Planet. Sci. Lett. 371–372, 143–155.
Sperling, E.A., Wolock, C.J., Morgan, A.S., Gill, B.C., Kunzmann, M., Halverson, G.P., Macdonald, F.A., Knoll, A.H., Johnston, D.T., 2015. Statistical analysis of iron geochemical data suggests limited Late Proterozoic oxygenation. Nature 523, 451–454.
Stouge, S., Christiansen, J.L., Harper, D.A.T., Houmark-Nielsen, M., Kristiansen, K., MacNiocaill, C., Buchardt-Westergård, B., 2011. Neoproterozoic (Cryogenian–Ediacaran) deposits in East and North-East Greenland. In: Arnaud, E., Halverson, G.P., Shields-Zhou, G. (Eds.), The Geological Record of Neoproterozoic Glaciations, Memoir 36. The Geological Society, London, pp. 581–592.
Strauss, J.V., Macdonald, F.A., Halverson, G.P., Tosca, N.J., Schrag, D.P., Knoll, A.H., 2015. Stratigraphic evolution of the Neoproterozoic Callison Lake Formation: linking the break-up of Rodinia to the Islay carbon isotope excursion. Am. J. Sci. 315, 891–944.
Strauss, J.V., Rooney, A.D., Macdonald, F.A., Brandon, A.D., Knoll, A.H., 2014. 740 Ma base-shaped microfossils from Yukon, Canada: implications for Neoproterozoic chronology and biostratigraphy 740 Ma vase-shaped microfossils from Yukon, Canada: implications for Neoproterozoic chronology and biostratigraphy. Geology 42, 659–662.
Swanson-Hysell, N.L., Maloof, A.C., Condon, D.J., Jenkin, G.R.T., Alene, M., Tremblay, M.M., Tesema, T., Rooney, A.D., Haileab, B., 2015. Stratigraphy and geochronology of the Tambien Group, Ethiopia: evidence for globally synchronous carbon isotope change in the Neoproterozoic. Geology 43, 323–326.
Swanson-Hysell, N.L., Maloof, A.C., Kirschvink, J.L., Evans, D.A.D., Halverson, G.P., Hurtgen, M.T., 2012. Constraints on neoproterozoic paleogeography and paleozoic orogenesis from paleomagnetic records of the bitter springs formation, central Australia. Am. J. Sci. 312, 817–884.
Swett, K., Knoll, A.H., 1985. Stromatolitic bioherms and microphytolites from teh late Proterozoic Draken Conglomerate Formation, Spitsbergen. Precambrian Res. 28, 327–347.
Swett, K., Knoll, A.H., 1989. Marine pisolites from Upper Proterozoic carbonates of East Greenland and Spitsbergen. Sedimentology 36, 75–93.
Tahata, M., Sawaki, Y., Yoshiya, K., Nishizawa, M., Komiya, T., Hirata, T., Yoshida, N., Maruyama, S., Windley, B.F., 2015. The marine environments encompassing the Neoproterozoic glaciations: evidence from C, Sr and Fe isotope ratios in the Hecla Hoek Supergroup in Svalbard. Precambrian Res. 263, 19–42.
Thomas, C.W., Graham, C.M., Ellam, R.M., Fallick, A.E., 2004. $^{87}Sr/^{86}Sr$ chemostratigraphy of Neoproterozoic Dalradian limestones of Scotland and Ireland: constraints on depositional ages and time scales. J. Geol. Soc., London 161, 229–242.
Thomson, D., Rainbird, R.H., Krapez, B., 2015a. Sequence and tectonostratigraphy of the Neoproterozoic (Tonian-Cryogenian) Amundsen Basin prior to supercontinent (Rodinia) breakup. Precambrian Res. 263, 246–259.
Thomson, D., Rainbird, R.H., Planavsky, N.J., Lyons, T.W., Bekker, A., 2015b. Chemostratigraphy of the Shaler Supergroup, Victoria Island, NW Canada: a record of ocean composition prior to the Cryogenian glaciations. Precambrian Res. 263, 232–245.
Tosca, N.J., Macdonald, F.A., Strauss, J.V., Johnson, D.T., Knoll, A.H., 2011. Sedimentary talc in Neoproterozoic carbonate successions. Earth Planet. Sci. Lett. 306, 11–22.
Wilson, C., Harland, W., 1964. The Polarisbreen Series and other evidences of late-Precambrian ice ages in Spitsbergen. Geol. Mag. 101, 198–219.
Wilson, C.B., 1958. The lower Middle Hecla Hoek rocks of Ny Friesland, Spitsbergen. Geol. Mag. 95, 305–327.
Wilson, C.B., 1961. The upper Middle Hecla Hoek rocks of Ny Friesland, Spitsbergen. Geol. Mag. 98, 89–116.